Available online at www.sciencedirect.com
ScienceDirect
Coordination Chemistry Reviews 251 (2007) 454–473
COORDINATION CHEMISTRY REVIEWS
www.elsevier.com/locate/ccr

Review

The Raman effect and its application to electronic spectroscopies in metal-centered species: Techniques and investigations in ground and excited states

Wesley R. Browne [a], John J. McGarvey [b,*]

[a] *Organic and Molecular Inorganic Chemistry, University of Groningen, Groningen, The Netherlands*
[b] *School of Chemistry & Chemical Engineering, Queen's University Belfast, Belfast BT5 9AG, Northern Ireland, UK*

Received 15 January 2006; accepted 26 April 2006
Available online 4 May 2006

Contents

* Corresponding author. Tel.: +44 28 9097 5450.
E-mail address: j.mcgarvey@qub.ac.uk (J.J. McGarvey).

doi:10.1016/j.ccr.2006.04.019

Abstract

In the decades since its discovery and somewhat limited early applications, Raman scattering has become the basis for the development of a variety of methods for probing molecular structure both in ground and electronically excited states. In this review, following a brief look at the underlying principles of the Raman and resonance Raman effects, the intention is to discuss a range of Raman techniques, especially in the context of their application to metal-centered systems. The review will focus on molecular electronic spectra, including bioinorganic examples, and on dynamic processes following electronic excitation. Methods to be surveyed will include continuous wave resonance Raman, surface-enhanced resonance Raman, time-resolved Raman and resonance Raman spectroscopies, which are used to probe the excited state processes, including vibrational dynamics, observed in molecular systems. The review will also include reference to coherent anti-Stokes Raman scattering, femtosecond coherent vibrational spectroscopy and time-resolved stimulated Raman spectroscopy on the femtosecond timescale.

Keywords: Raman; Time-resolved; Electronic; Coherence spectroscopy; Inorganic spectroscopy

1. Introduction

Raman spectroscopy has gone through several stages of development since the first reports of its experimental discovery in the late 1920s [1]. For many years however it remained something of an esoteric technique, based on the inelastic scattering of light, in which the filtered mercury arc excitation sources used in the early stages of its development necessitated accumulation over very lengthy exposure times to achieve acceptable signal levels. In the 80 years since its discovery and announcement, the Raman effect has experienced two periods of growth and widening of interest: (i) in the 1960s with the advent of the laser as an intense monochromatic light source; (ii) in the 1980s with advances in detector, filter and diode laser technology (Fig. 1) [2]. Indeed it is probably within the last two decades that the phenomenon of Raman scattering has seen its most rapid growth in popularity both in terms of the range of application to scientific problems and in the development of a number of techniques with Raman as a central feature for probing molecular structure, both in ground and electronically excited states.

In addition to taking a general overview of Raman scattering, the present review is intended to survey several more recently developed Raman techniques, including studies directed towards the femtosecond timescale and to place them in the context of the modern research environment. As a result of the breadth of the area being covered any attempt at a comprehensive treatment would be unrealistic and instead, the review will focus on selected investigations of the spectroscopy, photophysics and dynamics of metal-centered compounds, including those of bioinorganic interest, where Raman techniques are contributing to a more intimate understanding of ultrafast processes of chemical and biological interest. The review is directed, primarily, at researchers new to the field of Raman spectroscopy and consequently, in an attempt to make the review as self-contained as possible, it includes a brief account of the underlying principles of Raman and resonance Raman methods. Such an account does not purport in any way to replace the many excellent accounts of these topics, which are available in several textbooks and reviews [3], but rather should be viewed as a starting point for those who wish to explore the potential of Raman scattering, especially in its several recent guises, as an informative probe of molecular structure and dynamics.

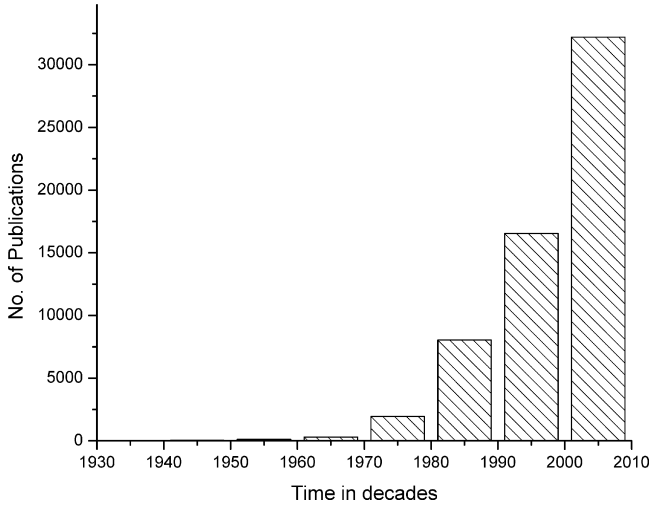

Fig. 1. Histogram of number of publications involving Raman and resonance Raman spectroscopy by decade.

1.1. Historical background

As with many areas of science the discovery of what is now known as the Raman effect is not without controversy. While Raman and Krishnan reported the first experimental study of inelastic light scattering in water and alcohol vapors in 1928 [1], the effect itself, the inelastic scattering of light by molecules, had already been predicted in the 1920s [4,5]. It is perhaps somewhat ironic that it was in water, the solvent of choice for Raman spectroscopy due to its intrinsically low Raman scattering cross-section and accompanying broad signals, that the effect was observed initially. Although the area received considerable academic attention in subsequent decades, technical limitations [6], in particular the requirement for monochromatic light sources and sensitive detectors, inhibited its development in favor of its complementary technique—infrared spectroscopy. The development of lasers in 1960s and more importantly, of multi-channel detectors in the 1970s led to renewed interest in Raman spectroscopy. In recent years the availability of charge coupled device (CCD and intensified gateable, iCCD) detectors, low cost, user friendly monochromatic light sources and single stage spectrometers coupled with holographic notch filters have led to a renaissance in Raman spectroscopy and it is now developing quickly into a routine spectroscopic technique, half a century after IR spectroscopy made a similar transition. Despite

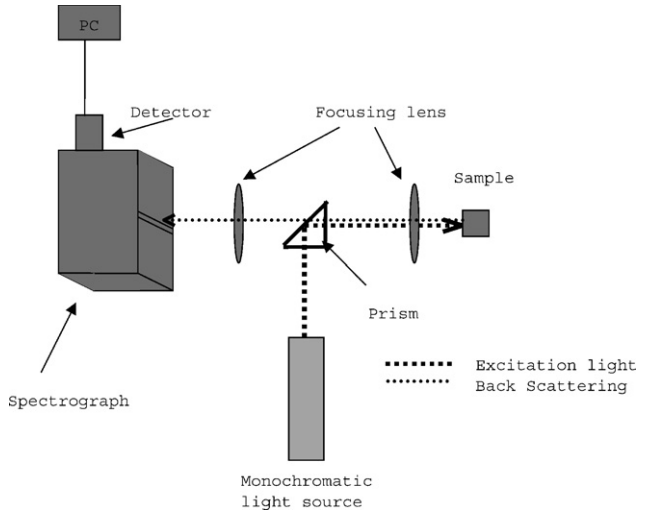

Fig. 2. Basic components of a Raman spectrometer. Although initially 90° scattering geometry was employed, most modern systems use a near back scattering geometry (135–180°), as depicted here.

the wide range of home-built and commercial Raman spectrometers available today, the simple, basic design has remained virtually unchanged and is outlined in Fig. 2.

1.2. Theoretical basis for Raman scattering

When monochromatic light impinges on a sample, much of it passes through the sample unchanged or some may be absorbed, depending upon the wavelength of the light and the nature of the sample. A small fraction, some 0.1%, is elastically scattered, as light of the same frequency as the incident light (Rayleigh scattering). An even smaller fraction of the incident light, perhaps amounting to 1 photon in 10^6 or 10^7, will be scattered inelastically (Raman scattering), either towards lower frequencies (Stokes scattering) or higher frequencies (anti-Stokes scattering), than the incident light. The differences in energy between the incident photons and inelastically scattered photons correspond to vibrational frequencies of the scattering molecule and the intensity is proportional to the fourth power of the scattered radiation, i.e. $(\bar{\nu} - \bar{\nu}_m)^4$ (Stokes) or $(\bar{\nu} + \bar{\nu}_m)^4$ (anti-Stokes) [7]. [N.B.: Throughout this review the frequency of Rayleigh or Raman scattered radiation will be expressed as a wavenumber (cm^{-1}), denoted $\bar{\nu}$ or $\bar{\nu}_m$, respectively.]

The essence of the Raman effect has been summarized by Myers [8] in sentences which could hardly be bettered: 'Spontaneous Raman signals are linear in the incident intensity but two photons are involved, one being spontaneously generated. In the traditional view of Raman scattering, a net vibrational transition is achieved through "virtual" excitation and de-excitation of higher energy states'. This is illustrated by the schematic energy level diagram in Fig. 3.

The scattering phenomenon may be described in terms of a simple quantum picture of energy exchange between the incident quantum of radiation and the scattering molecule. For an elastic collision involving no exchange of energy the frequency of the scattered photon remains unchanged, giving rise to Rayleigh scattering. In an inelastic collision, one possibility is that energy is transferred from the photon to the molecule, so that the photon will be scattered with lower energy and frequency (longer wavelength), giving rise to Stokes radiation. In the converse case, energy is transferred from the molecule to the photon, so that the scattered radiation is at higher frequency (shorter wavelength), so-called anti-Stokes radiation. In energy conservation terms, for an incident photon of wavenumber $\bar{\nu}$ (cm^{-1}), the inelastic scattering processes are represented by Eqs. (1) and (2):

$$hc\bar{\nu} = hc(\bar{\nu} - \bar{\nu}_m) + hc\bar{\nu}_m, \quad \text{Stokes scattering} \tag{1}$$

$$hc\bar{\nu} + hc\bar{\nu}_m = hc(\bar{\nu} + \bar{\nu}_m), \quad \text{anti-Stokes scattering} \tag{2}$$

where h is Planck's constant, c the velocity of light, $\bar{\nu}$ the frequency, expressed as a wavenumber (cm^{-1}) of the incident radiation, and $\bar{\nu}_m$ is the wavenumber equivalent to the energy difference between (usually) the lowest and first excited vibrational energy levels corresponding to one of the $(3N - 6)$ normal vibrational modes (not necessarily all 'Raman-active'—vide infra) of the scattering molecule. From a practical standpoint of spectroscopic observation, the important quantity is the Raman shift, $\bar{\nu} \pm \bar{\nu}_m$, of the scattered radiation from the incident radiation. Stokes scattering is generally more intense than anti-Stokes,

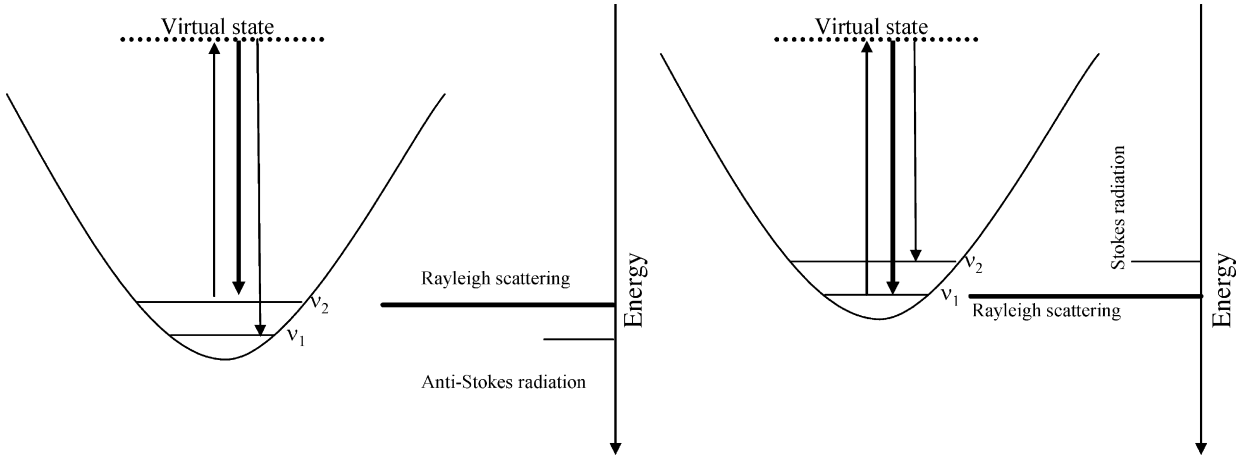

Fig. 3. Schematic representation of elastic (Rayleigh) and inelastic (right: Stokes and left: anti-Stokes) scattering involving a single vibrational mode.

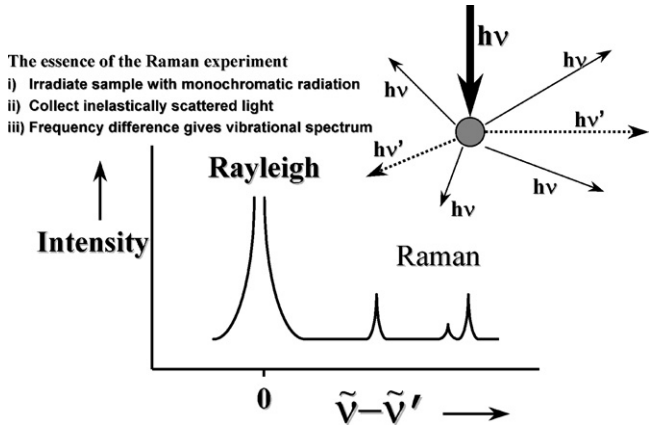

Fig. 4. Schematic representation of Rayleigh and Stokes Raman scattering. Dr. S.J. Bell is thanked for providing this figure.

primarily due to the Boltzmann distribution between the lowest vibrational states,

$$\frac{I_{\text{Stokes}}}{I_{\text{anti-Stokes}}} = \frac{(\bar{\nu} - \bar{\nu}_{\text{m}})^4}{(\bar{\nu} + \bar{\nu}_{\text{m}})^4} \exp\left(\frac{hc\bar{\nu}}{kT}\right) \tag{3}$$

and it is the Stokes Raman shift which is usually presented in a Raman spectrum, as shown schematically in Fig. 4.

A classical theory to explain the Raman effect and account for the principal selection rule involved commences with consideration of molecular polarisability. Polarisability describes the behavior of the electron cloud of the molecule in an electric field (E). The disturbance of the electron cloud induces an electric dipole moment (μ) and, hence, a polarisation of the molecule. The polarisability of a molecule determines the magnitude of the induced dipole moment [9]:

$$\mu = \alpha E \tag{4}$$

The electromagnetic field is itself dependent on the frequency ($\bar{\nu}$) of the incident light:

$$E = E_{\text{o}} \cos(2\pi\bar{\nu}ct) \tag{5}$$

where E_{o} is the incident electric field and t is time. Combining Eqs. (4) and (5) yields:

$$\mu = \alpha E_{\text{o}} \cos(2\pi\bar{\nu}ct) \tag{6}$$

which shows the relationship between the induced dipole moment and the frequency of the incident light. The oscillator will emit Rayleigh scattering radiation ($\bar{\nu}$). However, the polarisability changes with vibrational motion [10], Eq. (7).

$$\alpha = \alpha_{\text{o}} + \beta \cos(2\pi\bar{\nu}_{\text{m}}ct) \tag{7}$$

where α_{o} is the polarisability at the equilibrium position and β is $[\delta\alpha/\delta q]_{\text{o}}$, where q is the normal coordinate corresponding to a particular vibrational motion. Hence, Eq. (6) can be expanded to

$$\mu = \{\alpha_{\text{o}} + \beta(\cos 2\pi\bar{\nu}_{\text{m}}ct)\} E_{\text{o}} \cos(2\pi\bar{\nu}ct) \tag{8}$$

and hence to:

$$\mu = \underset{\text{Rayleigh}}{\alpha_{\text{o}} E_{\text{o}} \cos(2\pi\bar{\nu}ct)} + \frac{1}{2}\beta E_{\text{o}}(\underset{\text{anti-Stokes}}{\cos 2\pi[\bar{\nu} + \bar{\nu}_{\text{m}}]ct} - \underset{\text{Stokes}}{\cos 2\pi[\bar{\nu} - \bar{\nu}_{\text{m}}]ct}) \tag{9}$$

This equation embodies the important molecular selection rule for Raman scattering, i.e. the polarisability must change during the molecular (vibrational) motion, i.e. $\beta \neq 0$. Otherwise, the induced dipole oscillates only at the frequency of the incident radiation. If however the polarisability changes as a result of the vibrational motion, the second term in Eq. (9) containing β will be non-zero and hence Raman scattering will be observed.

With the possible exception of di- and tri-atomic molecules, deciding whether a particular vibrational mode is 'Raman-active' on the basis of the variation of the polarisability during the molecular vibration is not straightforward [11]. Fortunately, the Raman activity of any vibrational mode can be decided readily through the use of group theory, once the symmetry of the molecule under investigation has been assigned. Excellent accounts of the application of group theory in vibrational spectroscopy are available [12].

A quantity normally reported for the individual bands in a Raman spectrum is the depolarisation ratio, ρ, defined as the ratio, $I_{\perp}/I_{//}$, of the scattered Raman intensities with the electric vector perpendicular or parallel to the polarisation direction of the incident excitation laser radiation. For linearly polarised laser radiation, the ratio falls in the range: $0 \leq \rho \leq 3/4$. If $\rho \geq 0$ and <3/4 the corresponding band is 'polarised' and associated with a totally symmetric vibrational mode. If $\rho = 3/4$, the corresponding band is 'depolarised' and due to a non-totally symmetric mode.

1.3. Practical aspects of Raman spectroscopy

A key strength of Raman spectroscopy lies in its simplicity in terms of sample handling. Essentially the collection of Raman scattering requires that the sample is accessible to UV–vis radiation. In contrast to IR spectroscopy the 'vibrational' spectrum is generally observed in the UV–vis portion of the EM spectrum. In addition the collection of the scattered light is typically, though not necessarily, accomplished by means of ca. 180° back scattering arrangement (Fig. 2), eliminating the need for the sample to be transparent. As a result the arrangement for sampling is very versatile and even for samples which show very rapid photochemical decomposition, flow cells either under gravity or as a jet can enable good quality spectra to be recorded routinely. The use of notch filters and monochromators allows for detection of very low Raman shifts <100 cm^{-1}, and the advent of low-light measuring devices, electron-multiplying charge-coupled device detectors (EMCCDs), allow for much lower-powered lasers to be employed in spectral acquisition, a development of particular relevance to time-resolved techniques (vide infra) and more generally for the study of systems where sensitivity to light may be an issue.

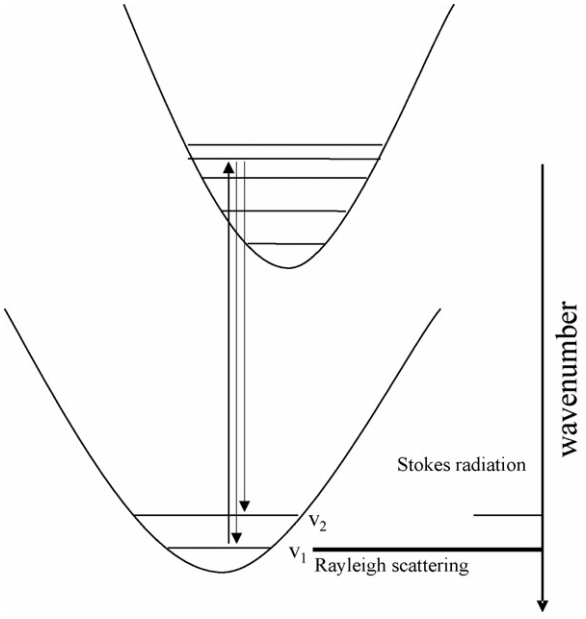

Fig. 5. Schematic diagram depicting resonance Raman scattering.

2. Resonance enhancement techniques

The resonance enhancement effect, i.e. the selective enhancement of Raman scattering when in 'resonance' with an electronic transition, so-called resonance Raman (rR) scattering, is one of the more remarkable and, with regard to the present review, one of the most useful aspects of Raman spectroscopy. The ability to enhance Raman scattering, often by more than six orders of magnitude, allows for the characterization of dilute solutions containing chromophoric species. Selective enhancement of scattering from particular vibrational modes provides detailed information as to the nature of electronic transitions. In the following sections, the origin of the resonance effect will be explored together with a brief introduction to the theoretical basis for our understanding of this effect (Fig. 5).

2.1. Resonance Raman scattering

An important practical consideration in the application of Raman scattering is its inherent weakness. However, when the wavelength of the incident light is coincident (i.e. resonant) with an electronic transition of the molecule then the Raman scattering observed may be enhanced by several orders of magnitude. However, the enhancement is not in general observed for all vibrational modes, rather certain modes become 'selectively' enhanced [13]. In fact, if the electronic transition in resonance with the Raman excitation wavelength is strongly allowed, then the vibrational modes which will be enhanced most strongly are the totally symmetric, Franck–Condon-active vibrational modes coupled with the electronic transition [8]. Two approaches for treating the rR phenomenon are the sum-over-states method [14] and the time-dependent wave packet theory [15]. The former is a classical time-independent approach involving Born–Oppenheimer separation of electronic and vibrational motions, while the latter adopts a dynamic view of the photon–molecule interaction. In the present general review it is not appropriate to enter into any detailed comparison between these methods, beyond some basic remarks, firstly regarding the sum-over-states approach which underlies the commonly presented discussion of the resonance Raman phenomenon. Some of the essential results from that approach will be used here. Detailed accounts are available elsewhere [8,16]. With regard to the wave packet theory, Myers [8] has pointed out that it provides much more satisfying insight into the link between resonance Raman intensities and excited state dynamics (see Section 6).

The key to understanding resonance Raman enhancement is to remember that the electronic transitions in a molecule are necessarily accompanied by vibrational energy changes (Fig. 6). Although an electronic transition in a molecule can be described as excitation from the ground electronic state $|g\rangle$ to an excited electronic state $|e\rangle$, in reality electronic and vibrational transitions are coupled and hence a better description of the process of absorption is excitation from a ground 'vibronic' state ($|i\rangle = |gm\rangle = |g\rangle|m\rangle$, where 'g' is the ground electronic state and 'm' is the initial vibrational state) to an excited 'vibronic' state ($|r\rangle = |ev\rangle = |e\rangle|v\rangle$, where 'e' is the excited – resonant – electronic state and 'v' is the vibrational state).

It should be noted that although the Raman scattering involves interaction with the excited electronic state ($|r\rangle$) the overall interaction results in a transition from the initial ($|i\rangle$) to the final ($|f\rangle$) vibronic states (where $|f\rangle = |g\rangle|n\rangle$). If $|m\rangle = |n\rangle$ then the interaction with light is elastic (no energy change, hence Rayleigh scattering); however, if $|m\rangle \neq |n\rangle$ then the scattered light will be either Stokes or anti-Stokes radiation.

We will now deliberately skip most of the mathematical detail and move to the essential result, which emerges from the sum-over-states approach, namely that the change in polarisability between the ground and excited electronic states is described by the polarisability tensor ($\alpha_{\rho\sigma}$) and that the two principal contributions to the tensor are referred to as the A and B terms [17].

$$[\alpha_{\rho\sigma}]_{\mathrm{if}} = A + B \tag{10}$$

where i: initial state and f: final state.

If the polarisability tensor is expressed as vibrational and electronic contributions (taking the sum-over-states approach), the A and B terms are given by Eqs. (11) and (12) [16a]:

$$A = \frac{1}{hc}[\mu_\rho]_{\mathrm{ge}}[\mu_\sigma]_{\mathrm{eg}} \sum_{\mathrm{v}} \frac{\langle n_{\mathrm{g}}|v_{\mathrm{e}}\rangle\langle v_{\mathrm{e}}|m_{\mathrm{g}}\rangle}{\bar{\nu}_{\mathrm{ev,gm}} - \bar{\nu}_0 + \mathrm{i}\Gamma_{\mathrm{ev}}} \tag{11}$$

$$B = \frac{1}{h^2c^2} \sum_{\mathrm{s}\neq\mathrm{e}} [\mu_\rho]_{\mathrm{gs}}[\mu_\sigma]_{\mathrm{eg}} \frac{h^k_{\mathrm{se}}}{\Delta\bar{\nu}_{\mathrm{se}}} \sum_{\mathrm{v}} \frac{\langle n_{\mathrm{g}}|Q_{\mathrm{k}}|v_{\mathrm{e}}\rangle\langle v_{\mathrm{e}}|m_{\mathrm{g}}\rangle}{\bar{\nu}_{\mathrm{ev,gm}} - \bar{\nu}_0 + i\Gamma_{\mathrm{ev}}} + \frac{1}{h^2c^2} \sum_{\mathrm{s}\neq\mathrm{e}} [\mu_\rho]_{\mathrm{ge}}[\mu_\sigma]_{\mathrm{sg}} \frac{h^k_{\mathrm{se}}}{\Delta\bar{\nu}_{\mathrm{es}}} \sum_{\mathrm{v}} \frac{\langle n_{\mathrm{g}}|v_{\mathrm{e}}\rangle\langle v_{\mathrm{e}}|Q_{\mathrm{k}}|m_{\mathrm{g}}\rangle}{\bar{\nu}_{\mathrm{eg,gm}} - \bar{\nu}_0 + i\Gamma_{\mathrm{ev}}} \tag{12}$$

where $\{s\}$ refers to other electronic excited states which interact with $\{e\}$ the resonant excited state. $[\mu_\rho]_{\mathrm{gs}} = \langle s|\mu_\rho|g\rangle$, the ρth term (x, y or z) of the electronic transition dipole moment for $|g\rangle \leftarrow |s\rangle$; $[\mu_\rho]_{\mathrm{ge}} = \langle e|\mu_\rho|g\rangle$, the ρth term (x, y or z) of the elec-

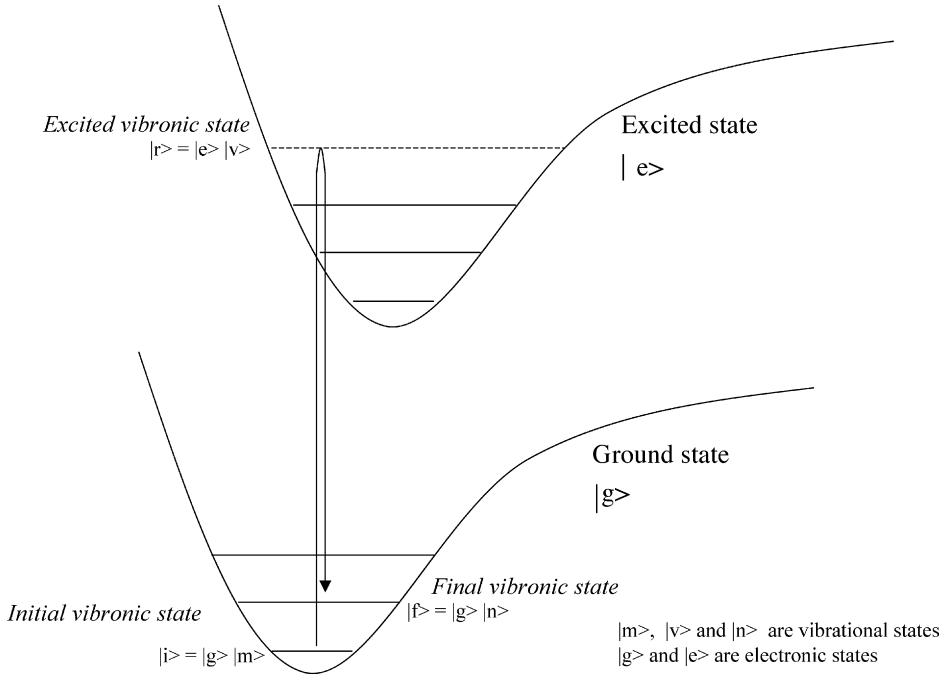

Fig. 6. Schematic diagram showing Resonance enhancement leading to Stokes Raman scattering.

tronic transition dipole moment for $|g\rangle \leftarrow |e\rangle$; $[\mu_\sigma]_{eg} = \langle e|\mu_\sigma|g\rangle$, the σth term (x, y or z) of the electronic transition dipole moment for $|e\rangle \leftarrow |g\rangle$; h^k_{se}: vibronic coupling integral {between the excited (e) state and a second excited electronic state (s)}; Q_k: the normal coordinates of the system; $\langle n_g|v_e\rangle\langle v_e|m_g\rangle$: products of vibrational overlap integrals (Franck–Condon factors); $i\Gamma_{ev}$: damping factor (cm^{-1}) (allowing for the fact that the electronic linewidth is finite [45]). $\bar{\nu}_{ev,gm} - \bar{\nu}_0$: wavenumber difference between the electronic transition and the laser excitation wavelength.

Hence, in order to achieve resonance enhancement of Raman scattering, either the *A* term or the *B* term (or both) must be non-zero. For the *A* term to be non-zero two criteria must be fulfilled, involving the vibrational and electronic contributions to the term. The electronic transition (i.e. the electronic absorption being used to achieve resonant enhancement) must be electric dipole allowed (i.e. $[\mu_\rho]_{ge}$ and $[\mu_\sigma]_{eg}$ not equal to zero). The second criterion is that the Franck–Condon factors $\langle n_g|v_e\rangle\langle v_e|m_g\rangle$ must not be equal to zero. This is the case when there is a change of shape between the ground and excited state potential wells or the excited state minimum is distorted with respect to the ground state (i.e. $\Delta Q > 0$, Fig. 7). Since the shift in ΔQ from the ground to the excited electronic state only occurs for totally symmetric vibrations (in the absence of molecular symmetry changes), it is only these modes which will undergo enhancement through the *A* term. The *B*-term involves coupling between the resonant and other electronically excited states and allows for scattering from non-totally symmetric modes to be enhanced.

2.2. Surfaced enhanced Raman spectroscopy

The first report of the observation of more intense Raman scattering in the vicinity of a surface was made by Fleischman et al. [18] in the mid-1970s, where unexpectedly intense Raman signals were obtained from pyridine monolayers on roughened silver electrodes. Although ascribed initially to the high surface concentration compared to the case with 'smooth' electrode materials, it was demonstrated later in two independent investigations that the increase in scattering intensity of up to 10^5 per pyridine molecule was actually due to the surface properties of the roughened electrode [19,20]. The mechanism for the surface-associated enhancement in Stokes scattering, now known generally as surface-enhanced Raman scattering (SERS), is still the subject of some debate. However, two models are accepted widely: (i) the charge transfer model and (ii) the electromagnetic model [21].

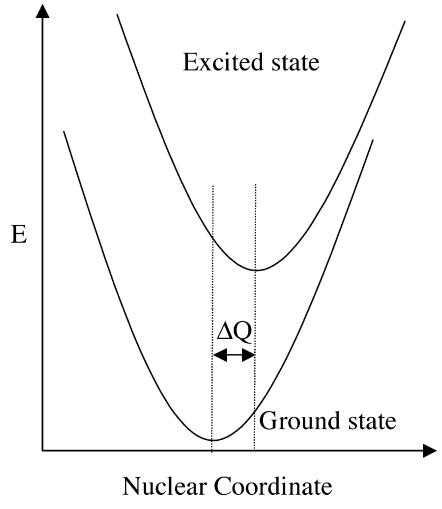

Fig. 7. Nuclear displacement between the ground and excited states (ΔQ).

As discussed above, the intensity of Raman scattering is dependent on the molecular polarisability (α) and the amplitude of the electric field (E). An increase in the magnitude of either α (charge transfer model) or E (electromagnetic model) will result in enhancement of the Raman scattering. The latter model, electromagnetic enhancement, involves interaction between molecules in the vicinity of a surface with surface plasmons (quantized oscillations of surface electrons) whose amplitudes are enhanced by interaction with light of a suitable wavelength. On a flat surface the energy is dissipated effectively as heat but at a rough surface some of the energy is re-emitted as radiation and if this radiation is resonant with the Raman and Rayleigh scatter of the adsorbed molecule then this scatter will be amplified.

The charge transfer model, involving a chemical interaction of the molecule with the surface, is based on an increase in molecular polarisability [22] of the adsorbed molecule by excitation of an electron from the surface into the LUMO of the adsorbed molecule. The electron tunnels back to the metal and the vibrationally excited neutral molecule relaxes to the ground state, emitting a photon as Raman scattering.

In practice SERS enhancement is achieved generally in one of two ways: (i) by aggregation of colloidal solutions of gold or silver in the presence of the analyte and (ii) by adsorption of the analyte at a roughened (nano-crystalline) metallic surface (usually gold and silver electrodes). Although an excellent method for obtaining Raman spectra of very small amounts of material [23], there are some disadvantages with the use of colloids as surfaces for SERS. Although the colloids can be prepared relatively routinely (albeit with a certain degree of art involved on the part of the chemist), they can give rise to non-reproducible SERS signals and, more importantly, are very sensitive to contamination.

2.3. Hyper Raman spectroscopy

Although currently of relatively minor interest for mainstream applications, another important enhancement process is the hyper Raman effect [24,25]. Resonance hyper Raman spectroscopy involves a two photon absorption process, a process which is of key importance in many areas of electronic spectroscopy including non-linear optics [24].

3. Dealing with fluorescence

A problem encountered frequently in practical Raman spectroscopy is that of fluorescence. In contrast to Raman scattering which is a very weak effect, luminescence is, frequently, characterized by quantum yields close to unity. Hence, the presence of fluorescence renders Raman spectral acquisition difficult at best. The simplest method of dealing with fluorescence is to avoid it, i.e. by selecting a wavelength region in which fluorescence is not observed. Unfortunately this approach is not always practical and alternative methods to deal with luminescence have been developed in recent years, including SERRS, SERDS and SSRS (vide infra), Kerr gating and anti-Stokes rR spectroscopy.

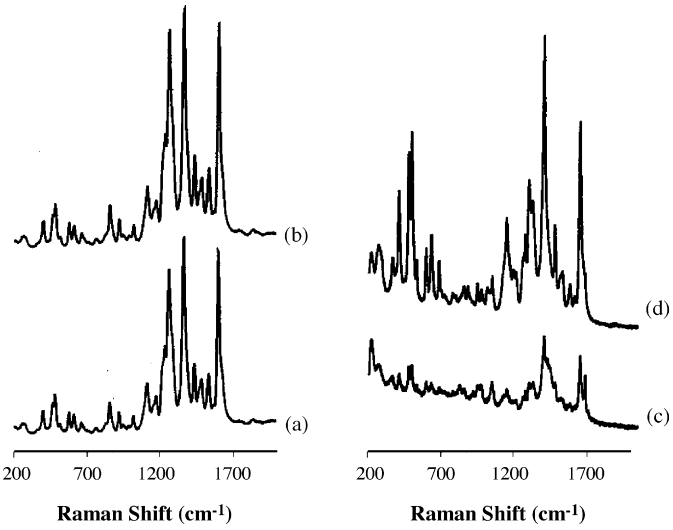

Fig. 8. SERS spectra of 4(5′-azobenzotriazoyl)-3,5-dimethoxyphenylamine on silver colloid at: (a) 457.9 nm, 5×10^{-8} M, (b) 457.9 nm, 5×10^{-7} M, (c) 632.8 nm, 5×10^{-8} M, and (d) 632.8 nm, 5×10^{-7} M. Absolute spectral intensities have been offset by an arbitrary amount in order to show the changes in relative intensity. Reproduced with permission from [26]. Copyright [2002] the American Chemical Society.

3.1. SERRS

The use of surface enhanced resonance Raman spectroscopy (SERRS) not only allows for resonance enhancement of the Raman scattering intensity but, frequently, the colloidal material used for the SERS enhancement can act to quench the luminescence also. This is perhaps the most frequently applied method for dealing with fluorescence of laser dyes [26]. It should be noted that in using SERS together with resonance enhancement the Raman spectrum obtained consists of scattering from vibrational modes which undergo enhancement and may suffer from some degree of irreproducibility as the contribution from the SERS and rR mechanisms may vary from measurement to measurement [26]. In addition, the mechanisms for SERS and SERRS enhancement appear to be different and the degree of particle aggregation important in the two techniques (Fig. 8).

3.2. Anti-Stokes Raman scattering

As mentioned above, anti-Stokes Raman scattering is much weaker than the more commonly employed Stokes Raman scattering. Despite this, interest in anti-Stokes Raman spectroscopy remains, due to the absence of interference by luminescence. Indeed Kitagawa and co-workers have employed anti-Stokes scattering very successfully in probing iron porphyrin complexes [27]. The inherent weakness of anti-Stokes radiation due to the very low Boltzmann population (Section 1.2) of higher lying vibrational levels can be overcome by vibrational excitation using infrared radiation. However, this approach can be frustrated by efficient vibrational relaxation, a point highlighted recently by Kitagawa and co-workers in the study of IR energy funneling in iron–porphyrin dendrimers [27].

In contrast to scattering from molecules in their electronic ground states, anti-Stokes scattering becomes more intense, and

hence more accessible, in vibrationally hot excited states. This aspect will be dealt with further in Section 5.

3.2.1. Coherent anti-Stokes Raman spectroscopy

The basis of the technique known as coherent anti-Stokes Raman scattering (CARS) spectroscopy lies in the use of two 'pump' laser beams. In this type of scattering spectroscopy when two ('pump') laser beams of wavenumbers $\bar{\nu}_1$ and $\bar{\nu}_2$ impinge on a sample, mixing may occur, giving rise to radiation of various frequencies including $\bar{\nu}_3 = \bar{\nu}_1 + (\bar{\nu}_1 - \bar{\nu}_2)$, fulfilling the conservation of energy requirement. When $(\bar{\nu}_1 - \bar{\nu}_2)$ corresponds to a Raman-active vibrational mode of the scattering molecule, coherent emission is observed, of wavenumber $\bar{\nu}_3$ and since this corresponds (from the conservation requirement) to the frequency of the anti-Stokes Raman line, the overall phenomenon is referred to as coherent anti-Stokes Raman scattering. The technique complements rR spectroscopy but shows enhanced signal:noise ratios and superior vibrational resolution. It can be applied in both continuous wave (CW) and time-resolved experiments. Sophisticated waveform fitting techniques are, however, required to extract the Raman spectra.

CARS has been used extensively to investigate biophysical systems such as visual pigments [28]. It has been applied to metal-centered species also, e.g. the investigation of the DNA-intercalating complex $[Ru(phen)_2dppz]^{2+}$ [29c] in which CARS was used to probe the extent of interaction of the complex in its ground state with DNA. This takes advantage of the high level spectral band resolution, $\sim 1\ cm^{-1}$, achievable through CARS. In addition, measurement of the vibrational spectra of the MLCT excited states of the complex becomes possible for comparison with independent TR^3 studies [30].

Another recent advance is the development of CARS microscopy, which evidently holds considerable promise for vibrational imaging in chemical and biological systems [31].

3.3. SERDS and SSRS

Subtracted shifted Raman spectroscopy (SSRS) [32] is a variation of shifted excitation Raman difference spectroscopy (SERDS) [33]. The technique involves acquiring a Raman spectrum (including background fluorescence) over as long a period as practical. If the Raman signal is strong enough to rise above the luminescent background, the latter can be subtracted as a baseline correction. However, the pixel to pixel response variation of a charge coupled device is ~1% and the signal may be similar in magnitude to the 'fixed pattern noise'. This situation can be overcome by recording two spectra in which either the excitation wavelength (SERDS) or the wavenumber position of the spectrograph (SSRS) is shifted between each acquisition of a spectrum. The fixed pattern noise in each spectrum will be at the same position; however, the Raman signal will be observed at different pixel numbers in each spectrum. Subtraction of the two

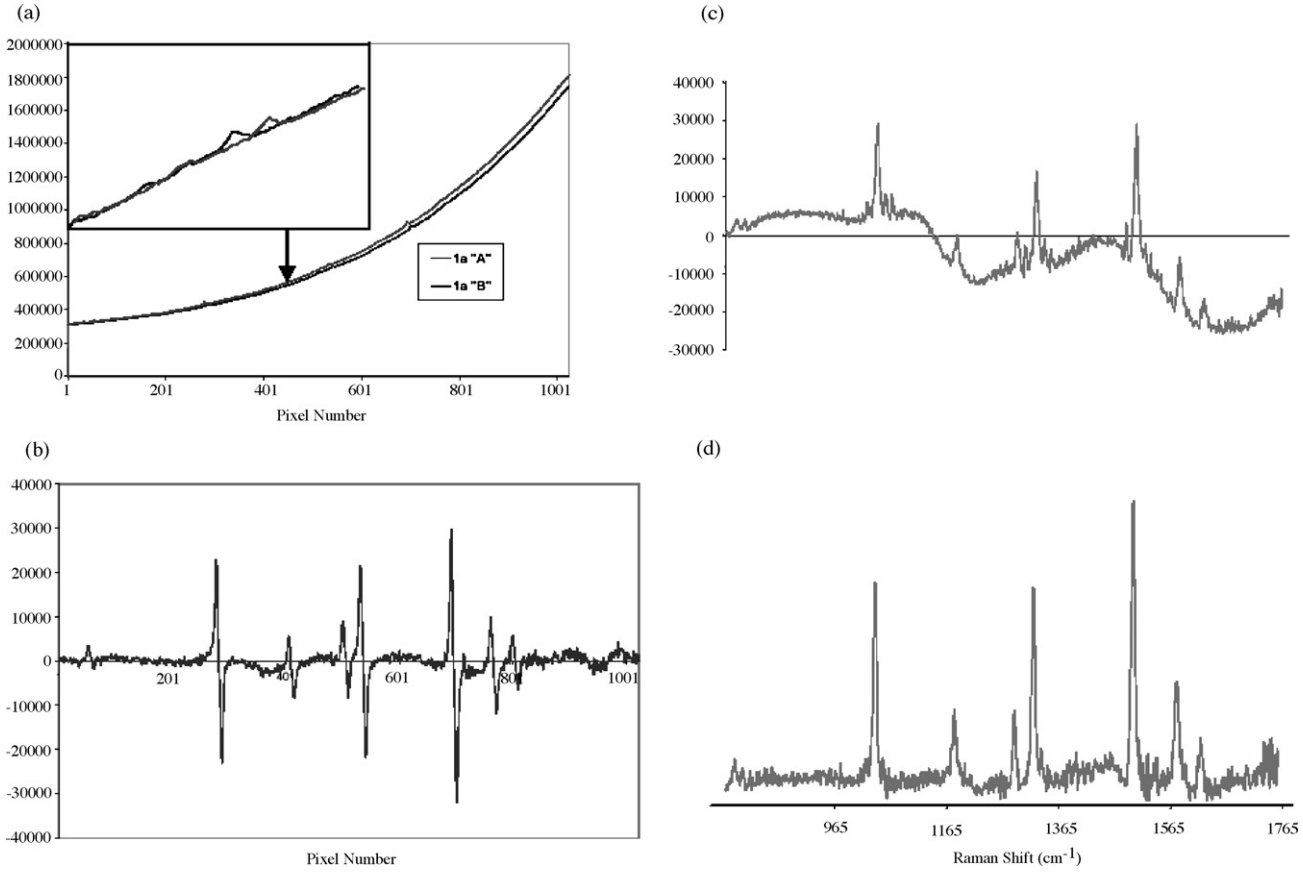

Fig. 9. Application of SSRS to the luminescent compound $[Ru(II)(bpy)(CN)_4]^{2-}$. $\lambda_{exc} = 488$ nm. Reproduced with permission from [34]. (a) Spectra A and B; (b) subtraction of spectra A and B; (c) mathematically reconstructed spectrum; (d) final spectrum.

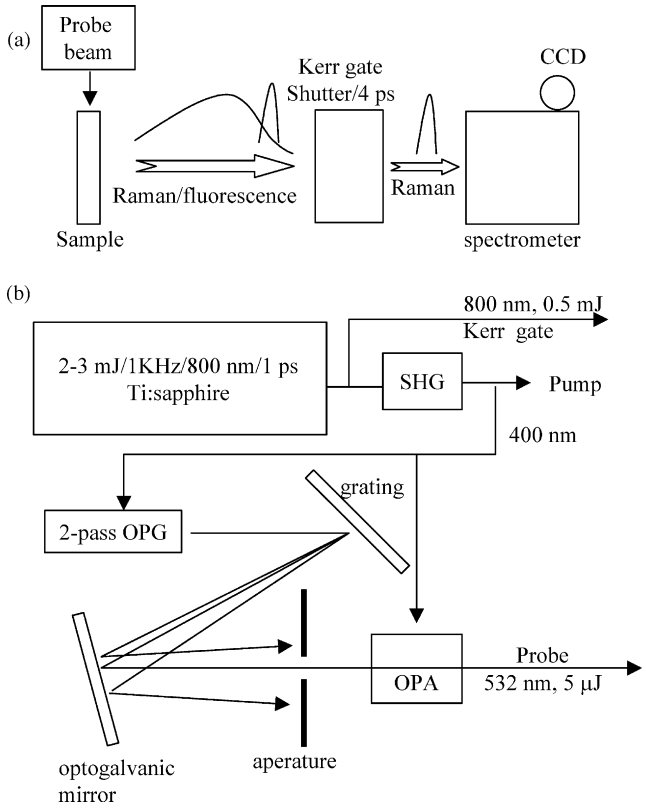

Fig. 10. (a) Principle of Kerr gated technique. (b) Schematic diagram of the laser setup for generation of pump, probe and pulse to open Kerr gate. Adapted from Matousek et al. [35]. Copyright John Wiley & Sons Limited. Reproduced with permission.

spectra will remove the fixed pattern noise and the luminescence but will result in a derivative like spectrum. Overall, SSRS holds some practical advantage over SERDS in that a tunable laser is required for the latter approach but only a spectrograph shift is required for SSRS. The latter technique has been applied to samples as diverse as drugs of abuse [32a] and ancient manuscripts [32b]. Fig. 9 shows an example of application of the technique to a luminescent metal complex [34].

3.4. Kerr gating

An alternative approach to dealing with background and sample fluorescence involves the use of the Kerr gate [35,36]. In essence, the Kerr gate is an optically driven shutter, in which a portion of the laser output is redirected to pass through a 'Kerr cell' simultaneously with the probe beam. It takes advantage of the instantaneous nature of Raman scattering in contrast to relatively slow emission of light as fluorescence and phosphorescence. It is based on the principle that if the detector only receives light during a very short laser pulse (e.g. 2 ps) then most of the fluorescence (often 100 ps to tens of nanoseconds in lifetime) does not reach the detector (Fig. 10). Although the performance of the Kerr gate was tested originally with organic systems [35], it was subsequently successfully employed to combat the adverse effects of fluorescence in TR^3 studies of metal-centered species [30b,37].

4. Application of Raman scattering to electronic spectroscopy

Raman spectroscopy, and in particular resonance Raman spectroscopy, has received considerable attention as a complementary technique to electronic spectroscopy. In the present section we provide a brief overview of some examples of contributions of Raman and especially resonance Raman scattering towards understanding the solution behavior of both inorganic and bioinorganic systems [29,38]. Although for many inorganic complexes often quite intense visible absorption bands are observed, the observation of resonance enhancement in the Raman spectra of the complexes is not guaranteed. Two factors should be noted. The enhancement effect, which is dependent upon excitation being coincident with an electronic absorption band, is observed only for vibrational modes which are coupled to the electronic transition; see Section 2.1. A second factor to bear in mind is the population of long lived excited states, which depletes the effective ground state concentration and hence scattering intensity [39].

The primary application of resonance Raman in transition metal systems is in the characterization of electronic transitions, and in particular towards understanding the interaction of metal centers with the ligands and with other proximal metal centers both in the ground and excited electronic states. An example of the use of resonance Raman spectroscopy to investigate spectral transitions in the near-red spectral region is provided by recent studies of mixed valence di-copper cryptates. Evidence for Cu–Cu bonding was obtained through investigation of Raman excitation profiles, as well as evidence for multiple conformational states involving the di-copper–ligand entity, $[Cu_2L]^{3+}$ [40].

Electron and energy transfer processes from electronically excited states are of continuing interest not least with regard to artificial light harvesting and photonic systems [41]. The considerable attention which Ru(II), Re(I) and Os(II) polypyridyl complexes have received over the last three decades [29] is perhaps only matched by that given to the biologically relevant heme based systems [42] and copper–sulfur proteins [43].

4.1. Biological heme systems

Numerous important studies based on resonance Raman spectroscopy have been conducted in the bioinorganic sphere, as, for instance, in its use to elucidate the molecular mechanisms of processes such as oxygen storage and transport, electron transfer, etc. Resonance Raman spectroscopy has been employed for over 30 years in the study of heme systems and indeed the area was sufficiently advanced by 1974 to prompt an important review by Spiro [44]. The application of Raman to heme containing peroxidases and gas sensory proteins has been reviewed recently by Howes and co-workers [45], Uchida and Kitagawa [46] and Spiro and Li [47].

An excellent account which covers many illustrative case studies is provided in the recent article by Ohta and Kitagawa [48]. One example is included here by way of illustration: in

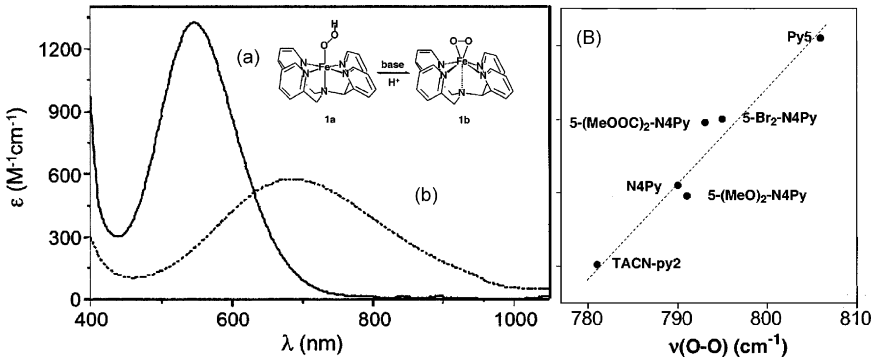

Fig. 11. (Left) Electronic absorption spectra of Fe(III)OOH and Fe(III)O_2 species formed by interaction of $[Fe(N4py)(CH_3CN)]^+$ with H_2O_2. (Right) Correlation between the redox potential of the Fe(II/III) redox couple of substituted $[Fe(N4py)(CH_3CN)]^+$ complexes and the μ(O—O) bond strength in their respective Fe^{III}–OOH complexes. Reproduced with permission from [49a]. Copyright [2003] American Chemical Society.

the well known process of CO binding to ferrous heme, rR spectroscopy in conjunction with isotopic substitution at the CO has been used to investigate the Fe–C–O geometry in a protein matrix by probing the stretching ($\bar{\nu}_{Fe-CO}$ and $\bar{\nu}_{C-O}$) and bending ($\bar{\nu}_{Fe-CO}$) vibrational modes associated with the iron–CO adduct. An unexpected observation was the occurrence of a higher bending, $\bar{\nu}_{Fe-C-O}$ (550–580 cm^{-1}), than stretching, $\bar{\nu}_{Fe-CO}$ (470–550 cm^{-1}), frequency. The effect was rationalized with the help of DFT calculations which suggested that the effect may be linked to steric and electrostatic barriers associated with the surrounding protein residues [48].

4.2. Oxidation catalysis

It is in the area of catalysis, both homo- and heterogeneous, that Raman spectroscopy offers an invaluable tool in understanding what are frequently quite complex and dynamic systems in matrices that are often far from ideal for spectroscopic analysis. The low concentrations of catalysts, anywhere between 5 and 0.01 mol%, with respect to the catalyst substrate and the use of non-aqueous solvents place considerable demands on the ability to 'see' the catalyst. The relatively broad features which are observed in the electronic spectra of the catalysts are often very useful in identifying inorganic complexes; however, resonance Raman can provide considerably more structural information such as the relative strength of metal-oxo bonds, etc. In addition the sensitivity to isotopic substitution and the generation of spectra by means of molecular modeling (i.e. DFT [21a]) often enables detailed analysis of the catalyst's state under reaction conditions.

Non-heme oxidation catalysts have been the focus of considerable attention over the last decade by Feringa, Que and co-workers and this is an area in which resonance Raman spectroscopy has proven to be of considerable benefit [49]. Of particular importance in these studies is the formation of iron(III) peroxy species (i.e. Fe^{III}–OOH and Fe^{III}–O_2^-) and high valent iron(IV) and iron(V) oxo species (i.e. Fe^{IV}=O and Fe^{V}=O). For these 'activated' complexes, of particular interest are the nature of the binding of the peroxy species to the iron and the relationship between bond strength and reactivity (Fig. 11). It is in addressing these two areas that rR spectroscopy has proven invaluable.

Similarly, resonance Raman has enabled the determination of the relative strength of Fe(IV)=O bonds in the complexes $[Fe^{IV}(O)$–$(TMC)(X)]^+$ (where TMC = 1,4,8,11-tetramethyl-1,4,8,11-tetraazacyclotetradecane and X = $^-$NCS or $^-N_3$) [50]. In contrast to the CH_3CN substituted complex, both the $^-N_3$ and $^-$SCN substituted complexes displayed a strong absorption at 400 nm. The assignment of the band at around 400 nm as a LMCT Fe(IV)=O band was made on the basis of the absence of any azide or isothiocyanate features in the rR spectrum and the use of isotopic labeling and is the first observation of such a band by rR (Fig. 12). This shows that substitution of the acetonitrile stabilizes this transition.

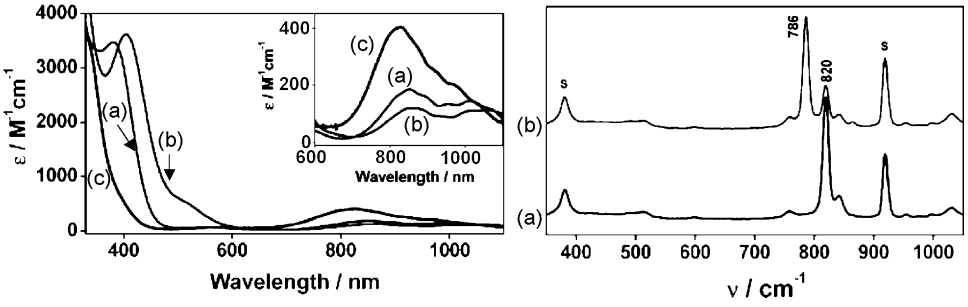

Fig. 12. (Left) UV–vis spectra of: (a) $[Fe^{IV}(O)(TMC)(NCS)]^+$, (b) $[Fe^{IV}(O)$–$(TMC)(N_3)]^+$ and (c) $[Fe^{IV}(O)(TMC)(NCCH_3)]^{2+}$. Inset shows the expanded near-IR absorptions. (Right) Resonance Raman spectra of: (a) $[Fe(^{16}O)(TMC)(NCS)]^+$ and (b) $[Fe(^{18}O)(TMC)(NCS)]^+$ in CH_3CN obtained at −20 °C with 406.7 nm excitation. The peaks marked with s are from solvent. Reproduced with permission from [50]. Copyright [2005] American Chemical Society.

4.3. Spectroelectrochemical Raman spectroscopy

A feature which has a significant bearing on the study of metal based systems in general is the frequent participation of several oxidation states. Essentially, Raman spectroelectrochemistry involves the generation of species in oxidation states which are normally not accessible synthetically [51].

4.3.1. Generation of anion radicals for comparison with electronically excited states

In Section 5 the use of Raman to investigate electronically excited states is discussed. Perhaps the most common excited state type encountered in investigations of inorganic complexes is the metal to ligand charge transfer (MLCT) state. MLCT states formally involve the transient single electron reduction of a ligand and oxidation of the metal center. The resonance Raman spectra of molecules in the MLCT state can, in principle, be approximated by generation of the one electron reduced ground state species, e.g. the ^{3}MLCT state of $[Ru^{II}(bpy)_3]^{2+}$ ($[Ru^{III}(bpy)_2(bpy^{*-}]^{2+}$) should resemble the reduced ground state $[Ru^{II}(bpy)_2(bpy^{*-}]^{+}$, although it has been pointed out that in such comparisons, sometimes caution needs to be exercised, such as in the case of $[Ru^{II}(phen)_3]^{2+}$. Comparison of the phen anion radical ($Li^{+}phen^{*-}$) with the optically generated ($[Ru^{III}(phen)_2(phen^{*-}]^{2+}$) suggested that the excited state in this complex is delocalized [52]. Comparison of the rR spectra of the electrochemically generated phen anion radical ($[Ru^{II}(phen)_2(phen^{*-}]^{+}$) with that of the optically generated ^{3}MLCT excited state ($[Ru^{III}(phen)_2(phen^{*-}]^{2+}$), however, pointed to the need for reinterpretation of the original studies to demonstrate that the excited state in this complex is localized, thus parallelling the case for its bpy analogue [53] (Fig. 13).

4.3.2. Exploring redox-dependent structural changes

The effect of reversible redox processes on the structure of inorganic systems such as Vanadyl-tetraphenylporphyrin can be probed using resonance Raman spectroscopy [54]. In this example, the effect of reduction of the porphyrin on the length of the V=O bond could be determined through rR spectroscopy. The rR spectrum of (O=V)TPP shows the presence of the O–V stretching mode for the neutral species, at 992 cm^{-1}, which undergoes a 12 cm^{-1} red-shift upon one electron reduction. The weakening of the V=O bond was ascribed to the localization of the electron in a porphyrin LUMO orbital involving the nitrogen donor atoms, increasing their donor strength and thereby weakening the V=O bond (Fig. 14).

4.3.3. Mixed valence systems

The area of mixed valence chemistry in binuclear complexes represents perhaps the most common application of inorganic spectroelectrochemistry. Recently the application of Raman spectroscopy to investigation of the nature of mixed valence species, i.e. the localized/delocalized nature of the singly occupied molecular orbital (SOMO), has received increasing attention [55].

The extent of localization of the SOMO in a binuclear complex in the mixed valence state {e.g. Ru(II)–BL–Ru(III), where BL is a bridging ligand} is usually classified as Type I, II, II/III or III (based on the classification proposed by Robin, Day, Hush and later, Meyer and co-workers) [56]. In symmetric binuclear complexes in which the SOMO is fully delocalized over the two metal centers (Type III) the vibrational structure (Raman spectrum) will be different to that of the fully oxidized or reduced states. By contrast, in fully localized systems (Type I), the vibrational spectrum of the mixed valence complex will be a superposition of the fully oxidized and reduced states. In the intermediate regime, i.e. type II systems where the SOMO is not completely delocalized or fast 'electron hopping' between the two metal centers occurs, then the situation becomes more interesting and the timescale becomes an important issue. In contrast to techniques such as NMR and EPR spectroscopy, where data are acquired typically in the micro- and millisecond domain, Raman scattering is instantaneous and hence the spectrum obtained will correspond to a Boltzmann distribution of species in several states.

4.4. Resonance Raman in the UV

The field of resonance Raman has, to a large extent, been dominated by studies in the visible region of the EM spectrum;

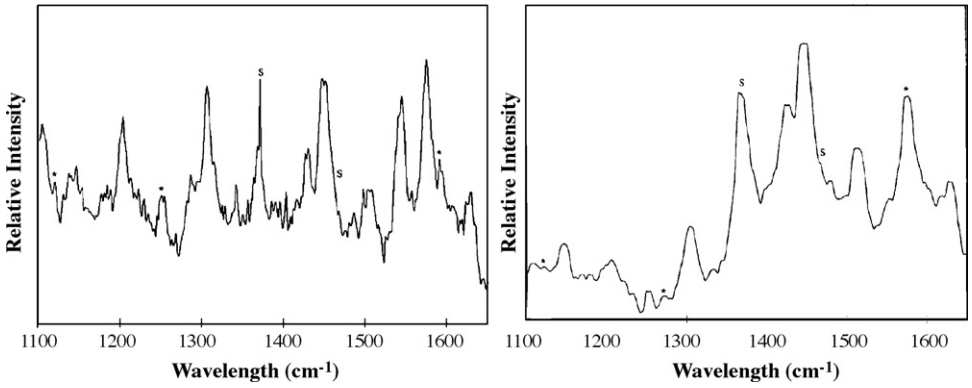

Fig. 13. (Left) rR of spectrum $[Ru(phen^{*-})(phen)_2]^{+}$ (406.7 nm excitation), ~3 mM in acetonitrile-d_3 at 298 K. (Right) TR^2 spectrum of $[Ru(phen)_3]^{*2+}$ (354.7 nm excitation and scattering, ~4 mJ per pulse), ~3 mM in acetonitrile at 298 K. Bands from $phen^{*-}$ are labeled with "*". Solvent bands appear at 1376 and ~1450 cm^{-1} and are labeled "S". Reproduced with permission from [53]. Copyright [1998] American Chemical Society.

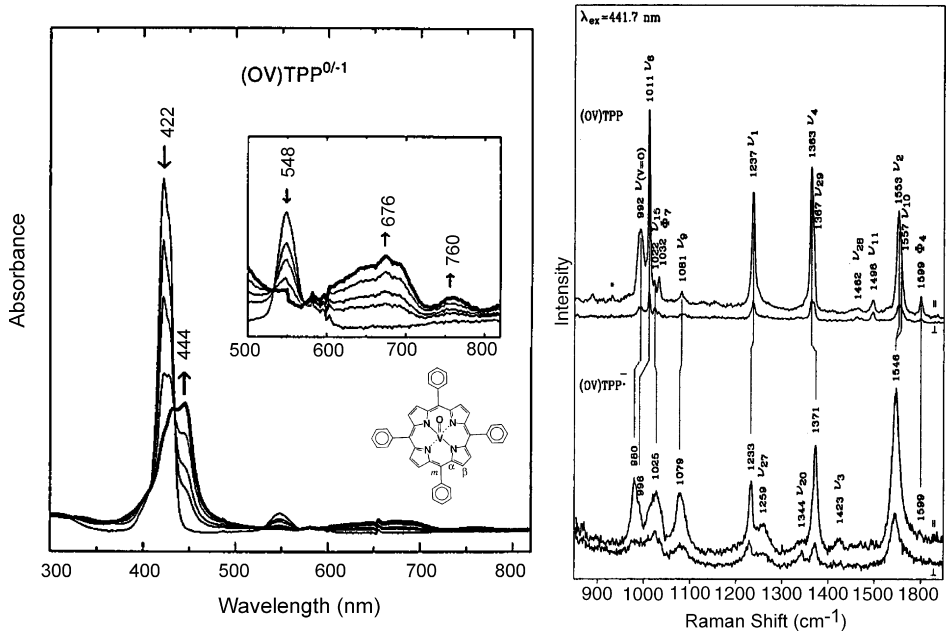

Fig. 14. (Left) UV–vis spectral changes upon reduction at −1.3 V vs. SCE. (Right) rR spectra of (V=O)TPP and its anion radical λ_{exc} = 441.7 nm in THF (solvent signals subtracted). The asterisk indicates the 934 cm^{-1} band of ClO_4^- (electrolyte). Applied potential −1.30 V vs. SCE. Reproduced from [54]. Copyright [1996] American Chemical Society.

however, more recently UV rR has seen an increase in popularity, with the advent of new generation pulsed lasers [57]. Several advantages of UV Raman are the very large spectral windows (in terms of wavenumber (cm^{-1})) over which measurements are possible, the avoidance of fluorescence (vide supra) and the very strong molar absorptivities normally encountered for analytes in this spectral region. It is perhaps in the study of DNA and protein dynamics that this technique will see widespread application in the near future, where UV rR can provide considerable information regarding the protein environment surrounding transition metal sites in metalloproteins [58].

5. Investigating excited state electronic structure

The investigation of the nature of electronically excited states is an area of intense scientific interest. In principle any spectroscopic technique can be employed to probe electronically excited states, provided of course that a significant concentration of excited state species can be maintained during the course of the data acquisition. The use of transient IR, UV–vis, EPR, etc., to probe excited states has been reviewed recently [64].

Raman and FTIR spectroscopy employing pulsed laser sources have proven invaluable in providing detailed information regarding excited state electronic structure and behavior [29b,59]. Although investigations of excited state behavior in transition metal systems have focused primarily on ruthenium(II) and rhenium(I) based polypyridyl complexes [60], other less accessible systems (i.e. non-emissive) have demonstrated the strength of transient resonance Raman spectroscopy. In the following section, basic experimental considerations in excited state Raman spectroscopy will be discussed with limited examples which illustrate the technique. First, however, it is useful to review several terms used in the literature:

Resonance Raman spectrum—Raman spectrum obtained with a light source (λ_{exc}) of wavelength coincident with an electronic absorption of the analyte.
Transient resonance Raman spectra TR^2—Raman spectra obtained using a single laser pulse to provide both excitation to electronically excited states and resonance Raman scattering from the prepared state.
Time-resolved resonance Raman spectra TR^3—The spectra of a transient or excited state species acquired by a probe laser pulse, at set time delays after generation by a ‘pump’ pulse. In such studies the pump and probe pulses may be of identical or different wavelengths, the choice obviously dependent upon the absorption spectra of the ground and excited state species under investigation.
Power-resolved TR^2—This is a remarkably useful technique and involves recording TR^2 spectra using a range of pulse powers. The higher the pulse power the larger the proportion of molecules that will be promoted to the excited state and hence the larger the contribution of excited state Raman scattering to the spectrum recorded and the lower the contribution of the ground state. See further comments in Section 5.1, especially in regard to incident photon:molecule ratios.
Excited state resonance Raman spectrum—Raman spectrum of a sample with a significant proportion of the sample in an electronically excited state.
Pure ground state spectrum—Spectrum showing only Raman signals of the analyte in the ground electronic state.

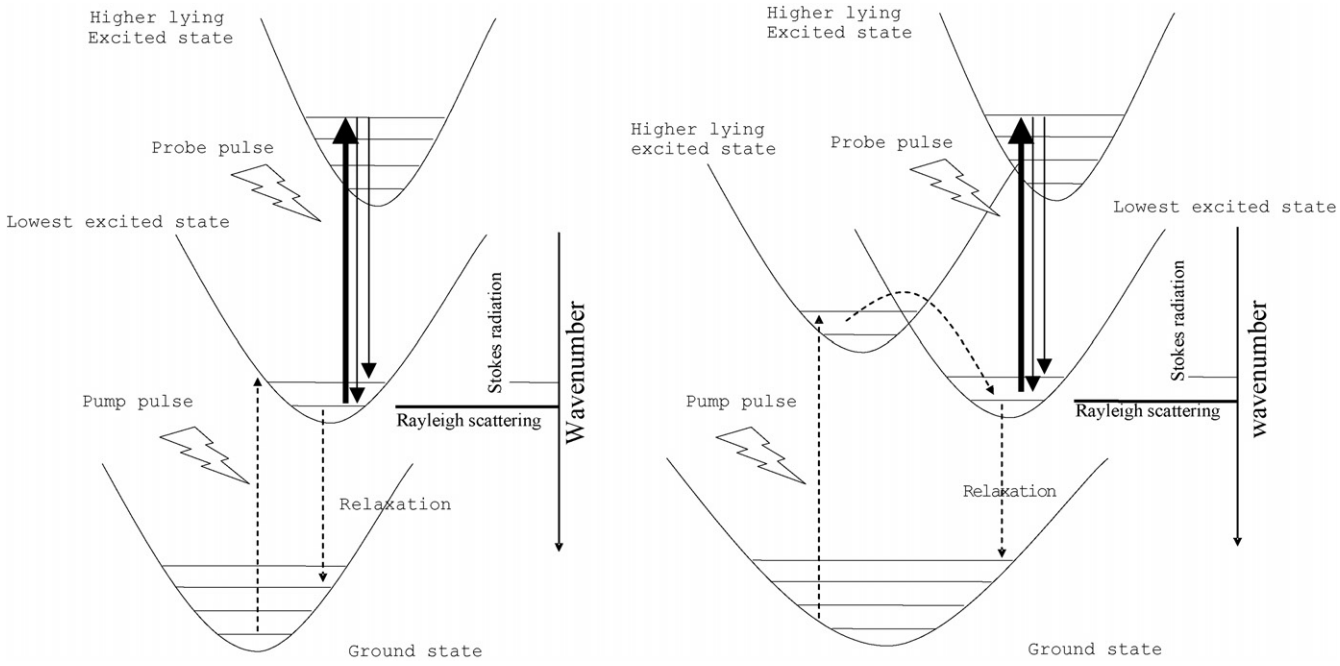

Fig. 15. Schematic diagram illustrating basic aspects of excited state resonance Raman spectroscopy (left: where the lowest excited state can be accessed directly by the pump pulse—more typical of organic systems; right: where the lowest excited state is not accessed directly—more typical of inorganic systems).

Pure excited state spectrum—Spectrum displaying only Raman signals of the analyte in the excited electronic state (ground state features have been removed by mathematical subtraction).

The basic excited state resonance Raman experiment is described (schematically) in Fig. 15. The experiment overall involves two photons of light. The first photon results in excitation to an excited state (pump pulse), with the second photon probing Raman scattering. This very simple description raises the issue of experimental requirements. Clearly, the pump pulse should be coincident with an electronic absorption of the ground state, while the probe pulse must be coincident with an electronic absorption of the excited state (established through transient absorption spectroscopy). If the latter requirement is not fulfilled, i.e. the excited state does not absorb at the probe wavelength, then as the power of the excitation pulse is increased the intensity of the Raman signals may actually decrease as the concentration of the analyte in the ground state becomes increasingly depleted.

5.1. Transient resonance Raman spectroscopy

By far the most accessible of excited state Raman techniques, TR^2 spectroscopy can provide a great deal of information regarding the nature of electronic excited states. The primary example of the use of transient resonance Raman spectroscopy to probe a metal-centered electronically excited states is found in the study of the paradigm complex $[Ru(bpy)_3]^{2+}$ by Woodruff, Dallinger and co-workers [61]. TR^2 enabled the identification of the lowest ^{3}MLCT state as involving electron localization on a single bpy ligand rather than delocalization over all three ligands. The basis for TR^2 is the use of a laser pulse to both 'pump' a significant proportion of absorbing molecules into an electronically excited state and probe the scattering from excited state molecules generated. Essentially the leading edge of the pulse is used to pump and the trailing edge to probe (i.e. generate Raman scattering from the populated species). It should be noted that there is an important difference between TR^2 spectra and pure excited state Raman spectra. The TR^2 spectrum is the spectrum obtained experimentally and includes Raman signals of the analyte in both the ground and excited states. By varying the power of the pulse the proportion of the sample pumped into the excited state can be varied and hence the relative intensities of the spectra of the electronically excited molecules and molecules in the ground state will vary. The mathematical subtraction of a lower power spectrum from a high power spectrum enables pure excited state spectra to be generated (and vice versa to generate the pure ground state spectrum). This process is demonstrated in Fig. 16.

Indeed, 'power-resolved' spectra can provide excited state resonance Raman spectra of systems, which have very short excited state lifetimes. This approach is illustrated elegantly, in the work of Caswell and Spiro in obtaining excited state rR spectra of the complex $[Ru(NH_3)_5(4,4'\text{-bpy})]^{2+}$ [62]. This complex has a very short excited state lifetime (<10–230 ps, depending on the protonation state) and hence when excited with a pulsed laser with FWHM of, in the case referred to, 10 ns, TR^3 spectra are not obtainable. Nevertheless, if the pumping rate is sufficiently high then a significant [detectable] proportion of the complex in the electronically excited state is maintained and is given by Eq. (13) [63]:

$$\frac{C^*}{C_o} = \frac{k_1}{k_1 + k_d} \tag{13}$$

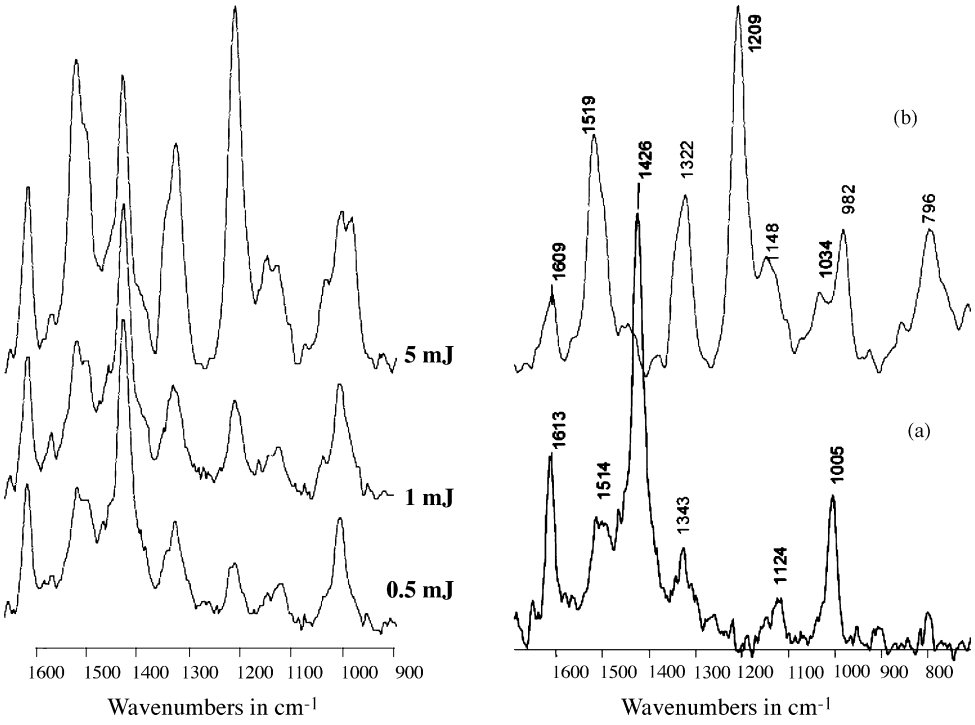

Fig. 16. (Left) Power dependence (0.5–5 mJ) in the spectra of $[(Ru(bpy)_2)_2(2,5\text{-bis}(5\text{-methyl-triazolato})pyrazine)]^{2+}$ in H_2O recorded in a single color (355 nm) TR^2 experiment. (Right) Pure ground (a) and pure excited state (b) spectra obtained by subtraction. Reprinted with permission from [65]. Copyright [2005] American Chemical Society.

where C^* is the concentration of species in the electronically excited state, C_o the analytical concentration of the compound, k_1 the pumping rate ($k_1 = \Phi \times (2.3 \times 10^3) \times \varepsilon \times I_o$, where Φ is the quantum yield of population of the excited state, ε the molar absorptivity of the ground state at the excitation wavelength and I_o is the intensity of the laser pulse in Einstein $cm^{-2}\ s^{-1}$) and k_d is the excited state decay rate.

5.2. Time-resolved resonance Raman

Time-resolved resonance Raman is an extension of the resonance Raman and transient resonance Raman experiments. As with TR^2 spectroscopy a pulse excitation source is employed to generate an electronically excited state, which is then probed using a second pulse of laser light. The second laser pulse is accompanied by gated detection (i.e. the detector shutter is only open when the second 'probe' pulse hits the sample) [64]. It is essential, however, that the probe pulse is sufficiently weak so as not to act as a 'pump' pulse itself.

There are two basic approaches to TR^3, (i) single color and (ii) two color. In the single color experiment a key problem is that during the cross-correlation time, i.e. when the pump and probe pulses overlap, Raman scattering from the pump pulse is detected as well as from the probe pulse. Although subtraction of 'pump only' spectrum can remove the contribution of the pump pulse, the subtraction is usually imperfect and subtle effects observed must be interpreted with considerable caution. The second approach, i.e. the two color approach, in principle avoids this problem as Raman scattering from the pump pulse is sufficiently removed (spectrally) from the probe Raman scattering that it will not be detected.

Frequently, in the literature what is referred to as time-resolved resonance Raman spectroscopy, is in fact TR^2—transient resonance Raman spectroscopy. Prior to the advent of picosecond and sub-picosecond excitation sources, the overwhelming majority of investigations fell into this latter category. A recent study on a pyrazine bridged binuclear ruthenium polypyridyl complex provides an example where both approaches, TR^2 and TR^3, were applied to advantage [65].

The information obtained from deuterium labeling and TR^2 studies on the dimeric complex $[(Ru(bpy)_2)_2(2,5\text{-bis}(5\text{-methyl-triazolato})pyrazine)]^{2+}$ (see Fig. 16) enabled assignment of the lowest ^{3}MLCT excited state as being pyrazine based. TR^3 studies of this complex were facilitated greatly by the electronic properties of the complex, which exhibits a very strong ground state absorption at 532 nm (the pump wavelength employed for the two color TR^3 experiments) and very strong excited state absorption at 354.5 nm (the probe pulse wavelength). Moreover, the complex is photostable in aqueous media. TR^3 spectra enabled confirmation that the pyrazine anion radical Raman bands decayed at a rate comparable to that of the luminescence lifetime of the complex. Furthermore, the decay in excited state signals and recovery of ground state signals was monotonic, showing that no additional processes were taking place (Fig. 17).

5.2.1. TR^3 in the picosecond–nanosecond region

Notwithstanding the discussion above, TR^3 can prove to be a very informative technique in understanding systems which show quite complex excited state dynamics. Before discussing

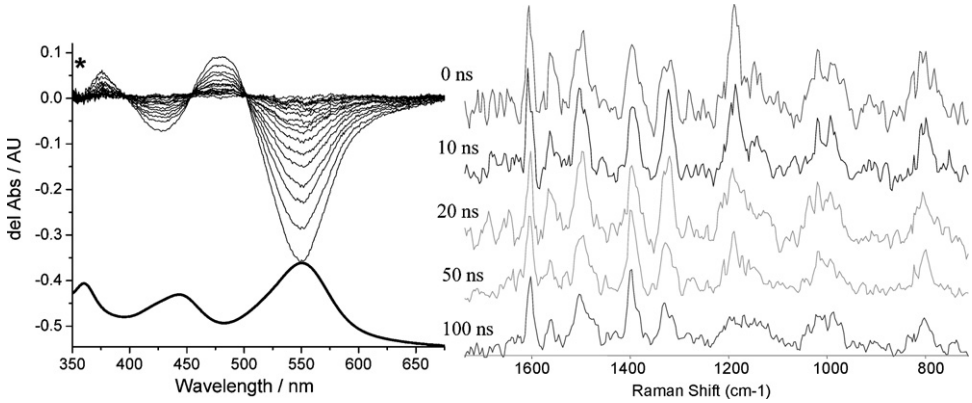

Fig. 17. (Left) Ground state (lower trace) and transient absorption difference spectra (upper traces) of $[(Ru(bpy)_2)_2(2,5\text{-bis}(5\text{-methyl-triazolato})pyrazine)]^{2+}$ (10 ns increment), $\lambda_{exc} = 450$ nm, '*' indicates 354.67 nm excitation line used in TR^2 and TR^3 experiments. (Right) TR^3 spectra of pyrazine bridged Ru(II) dimer in H_2O (ca. 10^{-3} M). Pump $\lambda = 532$ nm (10 mJ), probe $\lambda = 354.67$ nm (0.6 mJ). Spectra are normalized to 1398 cm^{-1} feature (ground state vibrational mode). Reprinted with permission from [65]. Copyright [2005] American Chemical Society.

transition metal based systems, however, it is appropriate to highlight an aspect of photophysics which has a bearing on Raman spectroscopy that is not always immediately apparent. The relaxation processes which follow excitation to the Franck–Condon state typically involve intersystem crossing and/or internal conversion processes. However, equally important is a process termed as vibrational relaxation or vibrational cooling. This process involves the loss of considerable amounts of vibrational energy to the solvent and hence the duration of the process shows a solvent dependence [66]. The importance of this process to TR^3 cannot be overstated as during this process the population of the excited state molecules in the lowest vibrational state (v = 1) is very low. Hence, the earliest recorded (picosecond timescale) resonance Raman spectrum of the lowest excited state may not reflect the time taken to populate that state from higher lying excited states. However, during this 'vibrationally hot' period the intensity of anti-Stokes Raman scattering is increased dramatically.

Although involving an organic system, an excellent example of the complementarity of Stokes and anti-Stokes Raman spectroscopy can be found in the picosecond time-resolved studies of the photochromic compound 1,2-bis(2,5-dimethyl-3-thienyl)perfluorocyclopentene [67]. This photochromic compound undergoes a 6π-electron ring closure reaction upon excitation of the 'open' state. The rate of the ring closure processes is generally accepted to be <4 ps [68]. However, the formation of the closed form detected by Stokes Raman spectroscopy could indicate the process is much slower (up to 10 ps, i.e. the time taken for the Raman signal at 1550 cm^{-1} to reach maximum intensity; Fig. 18(right)). The discrepancy between transient absorption (TA) and TR^3 data is rationalized by examination of the anti-Stokes Raman spectra, where a maximum in intensity is observed between 3 and 5 ps. The delay in the appearance of the Stokes Raman signals is therefore not due to a slow ring closure reaction, but rather due to quite slow vibrational cooling of the closed state itself. This example highlights a key point in examining excited state processes—comparison of timescales and effects should not be made without consideration of practical aspects of the experiments involved.

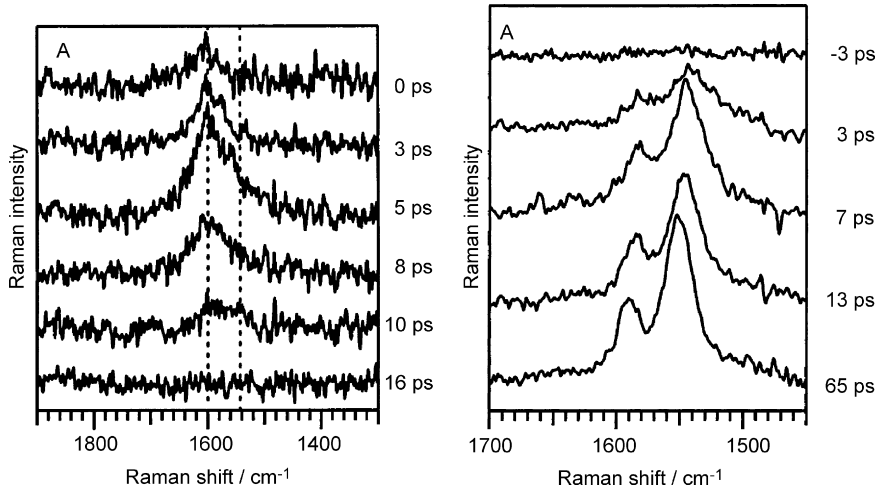

Fig. 18. Picosecond time-resolved anti-Stokes (left) and Stokes (right) spectroscopy following the photochemical cyclisation of 1,2-bis(2,5-dimethyl-3-thienyl)perfluorocyclopentene. Reprinted with permission from [67]. Copyright [2003] American Chemical Society.

A recent example of the ability of TR^3 to provide a deeper insight into systems which undergo excited state dynamics (from 1 ps to 100 ns in duration) can be found in the study of the spin-crossover systems $[Fe(btpa)]^{2+}$ (btpa = *N*,*N*,*N*′,*N*′-tetrakis(2-pyridylmethyl)-6,6′-bis(aminomethyl)-2,2′-bipyridine) and the predominantly low-spin species $[Fe(b(bdpa))]^{2+}$ ((b(bdpa) = *N*,*N*′-bis(benzyl)-*N*,*N*′-bis(2-pyridylmethyl)-6,6′-bis(aminomethyl)-2,2′-bipyridine) in solution [69]. In contrast to the pyrazine bridged binuclear ruthenium complex described above, these systems were far from ideal candidates for TR^3 experiments with relatively weak Raman signals being obtained. Nevertheless, a considerable body of information regarding the excited state dynamics of the complexes in solution could be obtained on both picosecond and nanosecond timescales, in particular regarding the low-spin, LS (^{1}A), to high-spin, HS (^{5}T), electronic spin-state crossover transition. For the nanosecond experiments, use of a probe wavelength at 321 nm, falling within the π–π^* transition of the polypyridyl backbone of the ligands, enabled the investigation of vibrational modes of both LS and HS isomers. The relaxation data from the nanosecond studies, in agreement with earlier transient absorption data [70], confirmed the biphasic spin-state relaxation in the case of $[Fe(btpa)]^{2+}$ and monophasic relaxation of $[Fe(b(bdpa))]^{2+}$. The picosecond results suggested an early process, which was complete within 20 ps, for both complexes.

6. Raman scattering in the femtosecond time domain—dealing with uncertainty!

In the previous section the application of Raman spectroscopy to the study of electronically excited states was explored. In particular, time-resolved resonance Raman spectroscopy has proven to be a highly informative structural probe over a broad time span, from milliseconds to picoseconds, covering much of the range of interest for chemistry and biological chemistry. It is clear that even in the picosecond time regime very detailed information can be obtained both from anti-Stokes as well as Stokes Raman spectroscopy. However, to probe the most intimate details concerning early stage dynamics and structural evolution of the nascent excited states requires investigations in the sub-pico- and femtosecond time regime, where Raman spectroscopy encounters the pulse length–bandwidth limit imposed by the Heisenberg Uncertainty Principle, which for practical purposes [71] translates into the requirement of a Raman excitation pulse duration of not less than ~1 ps, to maintain a Raman spectral band resolution of ~10–15 cm^{-1}.

One of the most exciting recent experimental developments in Raman spectroscopy, which 'circumvents' the uncertainty principle, has been the introduction of femtosecond time-resolved stimulated Raman spectroscopy (FSRS) [72–75]. Before discussing the details of the femtosecond stimulated Raman technique, several aspects of femtosecond coherence spectroscopy (FCS) [76,77], which enables the investigation of molecular vibrational oscillations on a sub-picosecond timescale, will be discussed. An account of the historical development of coherence spectroscopy, including reference to the earlier papers, is contained in the review by Polanyi and Zewail [78]. The question of sub-picosecond solvent dynamics in charge-transfer transitions in the context of resonance Raman band intensities has also been discussed [79].

6.1. Femtosecond coherence spectroscopy

Femtosecond coherence spectroscopy is a pump–probe technique that utilizes ultrafast laser pulses, shorter than the period of nuclear oscillations in molecules. Somewhat akin to the chemical relaxation approach used in the study of fast reactions, developed by Eigen in the 1950s [80], the underlying concept in FCS is to drive a sample out of equilibrium and then to follow its damped oscillatory response in real time [81].

As pointed out in an illuminating review by Nelson and co-workers [82], by working in the 'impulsive limit', i.e. the limit in which the pulse duration is less than a single vibrational oscillation period, phase-coherent vibrational motion can be initiated and monitored. The underlying basis of FCS is perhaps then a natural, albeit innovative, development of the use of ultrashort laser pulses. In the experimental strategy employed by the Champion group [81], pairs of laser pulses (each ca. 50 fs in duration) are used to pump and probe the sample, enabling real time observation of ultrafast processes, including the initial phases of the vibrational oscillations in the photoexcited species. Using this approach, Champion and co-workers have been able to distinguish between what they describe as 'field-driven' processes (in effect the Raman-active modes of the initially generated Franck–Condon excited state) and 'reaction-driven' processes, such as those involving electronic state surface crossings taking place away from the initial FC state. Thus, they have been able to detect and characterize in time-resolved fashion, low-frequency vibrational modes in heme proteins associated, apparently, with nuclear motion of the core of the porphyrin macrocycle [77]. The ability of FCS to distinguish 'field-driven' from 'reaction-driven' processes [81] was demonstrated more strikingly by the same group in studies of coherent vibrational oscillations in myoglobin, with the observation of an iron–histidine stretching mode in deoxymyoglobin, Mb, at 220 cm^{-1}. This mode is not active in the resonance Raman spectrum of MbNO, but is close to that observed in the rR spectrum of the deoxy-Mb, providing strong evidence that the FCS signals observed are generated by the electronic state changes accompanying ligand (NO) dissociation [76,83]. This work demonstrated a further advantageous feature of FCS also, namely its ability to probe low wavenumber vibrational modes, which would be too close to the Rayleigh line for detection by conventional time-resolved Raman methods. One other fascinating result highlighted by Champion et al. [83] is the extremely short timescale (much less than 150 fs) for the development of the ($S = 2$) high-spin product state of the iron atom in Mb from the initial unphotolyzed state ($S = 0$) of the six coordinate Mb–NO species. This is relevant to the related topic of electronic spin-state crossover in Fe(II) complexes, where there is growing experimental evidence of the $S = 2 \rightarrow S = 0$ transition occurring on a similar femtosecond timescale [89].

Thus, the technique can, in a number of instances, compete effectively with Raman spectroscopy. Indeed Champion and co-

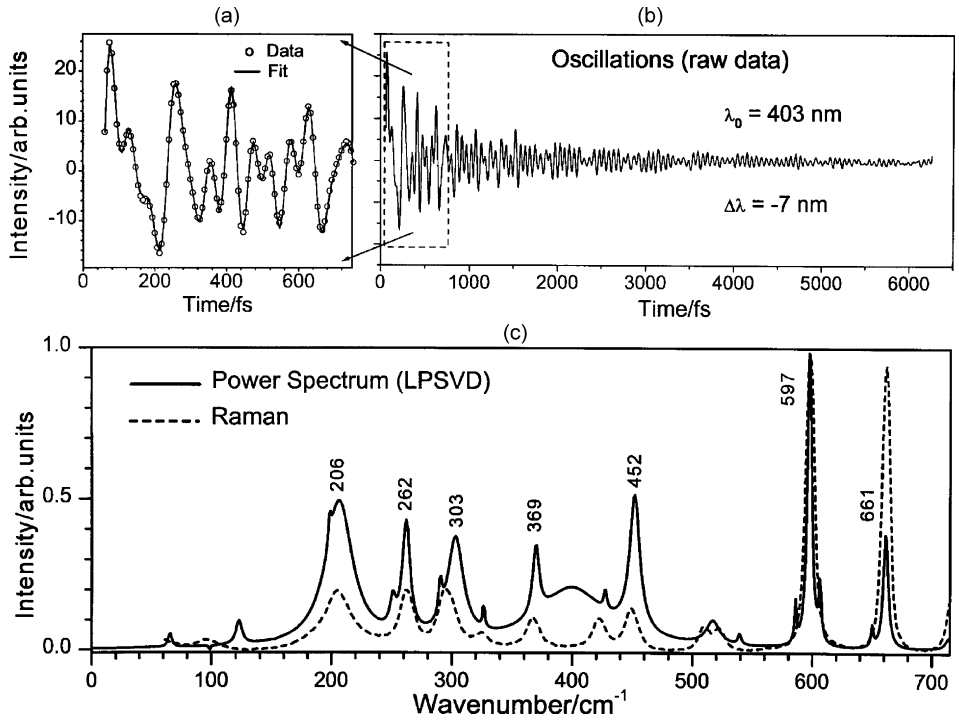

Fig. 19. Coherent oscillations in fenchone. (a) A detail of early time data (circles are the experimental points and the line is a linear prediction and singular value decomposition (LPSVD) fit); (b) the raw data; (c) results of the LPSVD fit in the form of a power spectrum (solid line) and fenchone Raman spectrum (dashed line). From Wang et al. [81]. Copyright John Wiley & Sons Limited. Reproduced with permission.

workers [81] have pointed out that FCS can be regarded as a time-domain analogue of Raman spectroscopy, in that the Fourier transform of the time-domain signal recovers a wavenumber 'energy-domain spectrum' that maps directly onto the traditional Raman spectrum. This mapping was illustrated by comparison of the ordinary Raman spectrum of fenchone (illustrated in Fig. 19 among other examples) with the coherent vibrational oscillations in the same liquid observed by FCS and analyzed to yield the power spectrum, analogous to a Fourier transform amplitude spectrum. Close agreement was found for the modes observable by FCS (limited by the bandwidth of the femtosecond laser pulses used).

6.2. Stimulated Raman spectroscopy

The concepts underlying stimulated Raman scattering have been considered in Section 3.2 in the context of the CARS technique, in which although the Raman scattering is coherent and much more intense than spontaneous (and incoherent) Raman scattering, the limitations of spectral and time resolution associated with the uncertainty principle still remain.

To address these problems the use of femtosecond stimulated Raman spectroscopy has been proposed by several groups [72,73,75]. In the detailed experimental approach described by the Mathies group [84] the FSRS technique enables the acquisition of resonance Raman spectra over a 1500 cm^{-1} window (vide infra), free from interference from fluorescence, with simultaneous high time (<100 fs) and frequency (ca. 15 cm^{-1}) resolution. The principles underlying the approach can be appreciated from Fig. 20 [72].

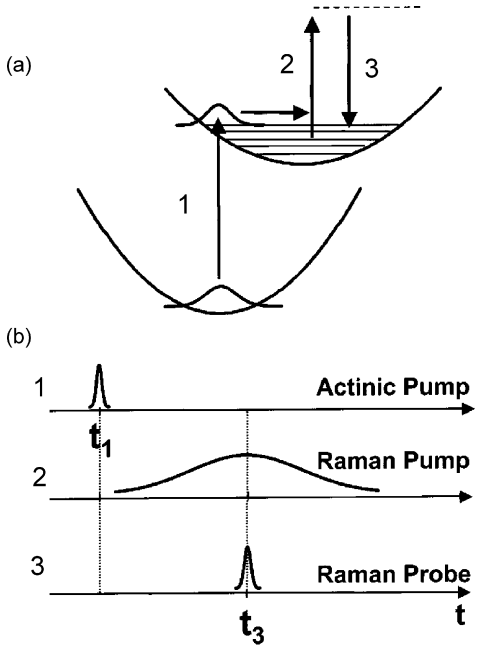

Fig. 20. Energy level diagram (a) and pulse timing schematic (b) for femtosecond stimulated Raman spectroscopy. The actinic pump pulse 1 excites the sample and initiates the photochemical events. The narrow band Raman pump pulse 2 and the broadband Raman probe pulse 3 arrive simultaneously. The resolution of the stimulated Raman spectrum imprinted on the Raman probe pulse is determined by the bandwidth of the Raman pump (~15 cm^{-1}). The collected Raman spectrum extends from 600 to 2100 cm^{-1}. The limiting time resolution is determined by the cross-correlation of the actinic pump and Raman probe pulses and is typically ~80 fs. Reproduced from [72] with permission of American Chemical Society (2003).

As can be seen from the figure, following photochemical initiation by a femtosecond (ca. 50 fs duration) pump (referred to as the 'actinic' pulse), two further laser pulses arrive simultaneously at the sample to drive the Raman transition: a picosecond 'Raman pulse' and a femtosecond broadband continuum 'probe pulse' that stimulates the scattering of any vibrational modes with frequencies between 600 and 2100 cm^{-1}. The latter range corresponds to the spectral limits of the probe pulse continuum generated in sapphire by the pump laser [84]. In effect, the experiment is operating at the 'impulsive limit' discussed earlier and enables the acquisition of very high time-resolved vibrational structural information that is not accessible to the incoherent, spontaneous Raman technique. The reliability of FSRS has been tested in several respects, such as its performance in fluorescence rejection in recording Raman spectra of fluorescent dyes and in time-resolved investigations, by applying it to probe ultrafast internal conversion in β-carotene and demonstrating that S_2–S_1 internal conversion occurred within 160 fs [72]. Much more recently the technique has been used to investigate the temporal sequencing of the geometric changes which occur in retinal within 200 fs of photoexcitation of rhodopsin [85]. In a revealing commentary [86] on this work, Champion notes that the experiment 'works' (i.e. there is no violation of the uncertainty principle) because the "gating" of the Raman coherence is controlled by changing the time delay between the photochemical ('actinic' in Fig. 20) pump and the broadband probe, thus allowing the dephasing time window to be moved. {Vibrational dephasing refers to the process whereby interaction of the excited species with the environment destroys the phase coherence of the system but leaves it in the original (i.e. unrelaxed) quantum state. Vibrational relaxation is a distinct process. The latter process and dephasing both contribute to the homogeneous linewidth [87].} This means that the rapid structural dynamics following excitation of the retinal chromophore to photorhodopsin and its decay to bacteriorhodopsin can be monitored.

It is clear that studies of this type are capable of providing much more detailed insight into how molecules, particularly those involved in photobiological processes, can channel the energy efficiently from initial photoexcitation into ultrafast structural changes. It is likely therefore that this very recent development will see application in many more areas in the future, including photoinduced heterogeneous charge injection and ultrafast energy transfer in molecular systems.

7. Conclusions and outlook

As stated at the outset, the primary intention of the present review is to provide an introduction to the basic principles underlying Raman and resonance Raman spectroscopy and to provide some illustrations of the power of these and more recently developed Raman-associated techniques for probing both electronically excited states and complex ground state processes in dynamic systems, especially where metal centers are involved. The pace of progress over the last 20 years can perhaps be appreciated from the title of a recent paper by Ishii and Hamaguchi [88]:

"Picosecond time-resolved multiplex CARS spectroscopy using optical Kerr gating"

This paper demonstrates both the level of sophistication achievable in Raman spectroscopy and also the modular nature of the techniques employed. The rapid technical developments with regard to instrumentation, not least in terms of detectors and laser sources, as well as the innovative and lateral thinking of spectroscopists, in addition to the rapid parallel advances in computational DFT techniques [48] will no doubt ensure the continued rapid expansion in all areas of (resonance) Raman spectroscopy.

References

[1] (a) C.V. Raman, R.S. Krishnan, Nature 121 (1928) 501;
(b) C.V. Raman, Indian J. Phys. 2 (1928) 387.

[2] (a) D.A. Long, Int. Rev. Phys. Chem. 7 (1989) 317;
(b) D. Bougeard, H. Hamaguchi, L.D. Ziegler, J. Raman Spectrosc. 34 (2003) 97.

[3] (a) J.R. Ferraro, K. Nakamoto, C.W. Brown, Introductory Raman Spectroscopy, second ed., Academic Press, Amsterdam, 2003;
(b) I.R. Lewis, H.G.M. Edwards, (Eds.), Handbook of Raman Spectroscopy, From the Research Laboratory to the Process Line, Marcel Dekker Inc., New York/Basel, 2001;
(c) A.B. Myers, Acc. Chem. Res. 30 (1997) 519;
(d) N.C. Craig, W.H. Fuchsman, N.N. Lacuesta, J. Chem. Educ. 80 (2003) 1282;
(e) D.A. Long, The Raman Effect: A Unified Treatment of the Theory of Raman Scattering by Molecules, 1st Ed., John Wiley & Sons, London, 2002.

[4] When studying the interaction of radiation with matter, Smekal predicted the possibility of light scattering occurring, which involved a change in energy of the scattering system. Kramers and Heisenberg and later Dirac, further developed this idea in the quantum theory of radiation and dispersion, respectively.

[5] K.S. Krishnan, in: A. Anderson (Ed.), The Raman Effect, Marcel Dekker Inc., New York, 1971, p. 5.

[6] The only suitable excitation source for Raman spectroscopy was the mercury arc lamp which restricted the choice of excitation wavelength (and hence the samples which could be studied) and its relatively low power output, which required large sample volumes and lengthy exposures of the photographic plates employed to detect the scattered radiation.

[7] G. Turrell, in: G. Turrell, J. Corset (Eds.), Raman Microscopy, Developments & Applications, Academic Press (Harcourt Brace & Company), London/New York, 1996 (Chapter 1).

[8] A.B. Myers, Acc. Chem. Res. 30 (1997) 519.

[9] To simplify the present treatment, the tensor properties of α are not discussed here. The interested reader is referred to Refs. [3e,7].

[10] Rotational motion should be considered, also.

[11] R.S. Tobias, J. Chem. Educ. 44 (1967) 1.

[12] (a) N.C. Craig, N.N. Lacuesta, J. Chem. Ed. 81 (2004) 1199;
(b) F.A. Cotton, Chemical Applications of Group Theory, third ed., Wiley/Interscience, New York, 1990.

[13] A.Y. Hirakawa, M. Tsuboi, Science 188 (1975) 359.

[14] C. Sourisseau, J. Chim. Phys. Phys.-Chim. Biol. 90 (1993) 1557.

[15] E.J. Heller, Acc. Chem. Res. 14 (1981) 368.

[16] (a) R.J.H. Clark, T.J. Dines, Angew. Chem. Int. Ed. Engl. 25 (1986) 131;
(b) A.M.J. Kelley, Phys. Chem. A 103 (1999) 6891;
(c) A.B. Myers, in: A.B. Myers, T.R. Rizzo (Eds.), Laser Techniques in Chemistry, Wiley, New York, 1995, p. 325;
(d) A.B. Myers, J. Raman Spectrosc. 28 (1997) 389.

[17] K. Nakamoto, J.R. Ferraro, Introductory Raman Spectroscopy, Academic Press Limited, 1994, p. 370.

[18] M. Fleischmann, P.J. Hendra, A.J. McQuillan, Chem. Phys. Lett. 26 (1974) 163.

[19] M.G. Albrecht, J.A. Creighton, J. Am. Chem. Soc. 99 (1977) 5216.
[20] D.I. Jeanmarie, R.P. Van Duyne, J. Electroanal. Chem. 84 (1977) 1.
[21] (a) B.D. Alexander, T.J. Dines, J. Phys. Chem. B 109 (2005) 3310;
(b) A. Otto, J. Raman Spectrosc. 36 (2005) 497;
(c) R.L. Garrell, Anal. Chem. 61 (1989) A401;
(d) A. Campion, P. Kambhampati, Chem. Soc. Rev. 27 (1998) 241;
(e) G.C. Schatz, Acc. Chem. Res. 17 (1984) 370;
(f) M. Kerker, Acc. Chem. Res. 17 (1984) 271.
[22] P. Kambhampati, C.M. Child, M.C. Foster, A. Campion, J. Chem. Phys. 108 (1998) 5013.
[23] (a) S. Nie, S.R. Emory, Science 275 (1997) 1102;
(b) K. Kneipp, Y. Wang, H. Kneipp, L.T. Perelman, I. Itzkan, R.R. Dasani, M.S. Feld, Phys. Rev. Lett. 78 (1997) 1667.
[24] For a detailed mathematical and experimental treatment of the hyper Raman effect see;
(a) L.C.T. Shoute, M. Blanchard-Desce, A. Myers Kelley, J. Phys. Chem. A 109 (2005) 10503, and references therein;
(b) L.D. Ziegler, J. Raman Spectrosc. 21 (1990) 769.
[25] M. Mizuno, H.O. Hamaguchi, T. Tahara, J. Phys Chem. A 106 (2002) 3599.
[26] C. McLaughlin, D. Graham, W.E. Smith, J. Phys. Chem. B 106 (2002) 5408.
[27] Y.J. Mo, D.L. Jiang, M. Uyemura, T. Aida, T. Kitagawa, J. Am. Chem. Soc. 127 (2005) 10020.
[28] G.H. Atkinson, Y. Zhou, L. Ujj, A. Aharoni, M. Sheves, M. Ottolenghi, J. Phys. Chem. A 106 (2002) 3325.
[29] (a) K. Nakamoto (Ed.), Infrared and Raman Spectra of Inorganic and Coordination Compounds, Part A: Theory and Applications in Inorganic Chemistry, John Wiley & Sons, Inc., New York, 1997;
(b) J.R. Schoonover, C.A. Bignozzi, T.J. Meyer, Coord. Chem. Rev. 165 (1997) 239;
(c) W.R. Browne, J.J. McGarvey, Coord. Chem. Rev. 250 (2006) 1696.
[30] (a) L. Ujj, C.G. Coates, J.M. Kelly, P.E. Kruger, J.J. McGarvey, G.H. Atkinson, J. Phys. Chem. B 106 (2002) 4854;
(b) C.G. Coates, J. Olofsson, M. Coletti, J.J. McGarvey, B. Onfelt, P. Lincoln, B. Norden, E. Tuite, P. Matousek, A.W. Parker, J. Phys. Chem. B 105 (2001) 12653.
[31] J.-X. Cheng, X.S. Xie, J. Phys. Chem. B 108 (2004) 827.
[32] (a) S.E.J. Bell, E.S.O. Bourguignon, A.C. Dennis, Analyst 123 (1998) 1729;
(b) S.E.J. Bell, E.S.O. Bourguignon, A.C. Dennis, J.A. Fields, J.J. McGarvey, K.R. Seddon, Anal. Chem. 72 (2000) 234;
(c) S.E.J. Bell, E.S.O. Bourguignon, A. O'Grady, J. Villaumie, A.C. Dennis, Spectrosc. Eur. 14 (2002) 17.
[33] N.J. Cherepy, A.P. Shreve, L.J. Moore, S. Franzen, S.G. Boxer, R.A. Matthias, J. Phys. Chem. 98 (1994) 6023.
[34] K.L. Ronayne, Ph.D. Thesis, Queen's University Belfast, Northern Ireland, 2004 (Chapter 4).
[35] P. Matousek, M. Towrie, A.W. Parker, J. Raman Spectrosc. 33 (2002) 238.
[36] P. Matousek, M. Towrie, A. Stanley, A.W. Parker, Appl. Spectrosc. 53 (1999) 1485.
[37] J. Olofsson, B. Onfelt, P. Lincoln, B. Norden, P. Matousek, A.W. Parker, E. Tuite, J. Inorg. Biochem. 91 (2002) 286.
[38] (a) J.H. Hibben, Chem. Rev. 13 (1933) 345;
(b) R.J.H. Clark, T.J. Dines, Angew. Chem. 98 (1986) 131.
[39] For example: obtaining ground state resonance Raman spectra for the paradigm complex $[Ru(bpy)_3]^{2+}$ at 363 nm, in the absence of excited state features, is almost, albeit not completely, impossible!.
[40] (a) A. Al-Obaidi, G. Baranovic, J. Coyle, C.G. Coates, J.J. McGarvey, V. McKee, J. Nelson Inorg. Chem. 37 (1998) 3567;
(b) S. Franzen, V.M. Miskowski, A.P. Shreve, S.E. Wallace-Williams, W.H. Woodruff, M.R. Ondrias, M.E. Barr, L. Moore, S.G. Boxer, Inorg. Chem. 40 (2001) 6375.
[41] M. Hang, V. Huynha, D.M. Dattelbaum, T.J. Meyer, Coord. Chem. Rev. 249 (2005) 457.
[42] D.H. Murgida, P. Hildebrandt, Acc. Chem. Res. 37 (2004) 854.
[43] C.R. Andrew, J. Sanders-Loehr, Acc. Chem. Res. 29 (1996) 365.
[44] T.G. Spiro, Acc. Chem. Res. 7 (1974) 339.
[45] G. Smulevich, A. Feis, B.D. Howes, Acc. Chem. Res. 38 (2005) 433.
[46] T. Uchida, T. Kitagawa, Acc. Chem. Res. 38 (2005) 662.
[47] T.G. Spiro, X.-Y. Li, in: T.G. Spiro (Ed.), Biological Applications of Raman Spectroscopy, vol. 3, John Wiley and Sons, New York, 1988, p. 1.
[48] T. Ohta, T. Kitagawa, Inorg. Chem. 44 (2005) 758.
[49] (a) G. Roelfes, V. Vrajmasu, K. Chen, R.Y.N. Ho, J.-U. Rohde, C. Zondervan, R.M. la Crois, E.P. Schudde, M. Lutz, A.L. Spek, R. Hage, B.L. Feringa, E. Muenck, L. Que Jr., Inorg. Chem. 42 (2003) 2639;
(b) R.Y.N. Ho, L. Que Jr., G. Roelfes, B.L. Feringa, R. Hermant, R. Hage, Chem. Commun. (1999) 2161;
(c) R.Y.N. Ho, G. Roelfes, B.L. Feringa, L. Que Jr., J. Am. Chem. Soc. 121 (1999) 264.
[50] C.V. Sastri, M.J. Park, T. Ohta, T.A. Jackson, A. Stubna, M.S. Seo, J. Lee, J. Kim, T. Kitagawa, E. Muenck, L. Que Jr., W. Nam, J. Am. Chem. Soc. 127 (2005) 12494.
[51] (a) R.T. Packard, R.L. McCreery, Anal. Chem. 59 (1987) 2631;
(b) A. Bonifacio, D. Millo, C. Gooijer, R. Boegschoten, G. van der Zwan, Anal. Chem. 76 (2004) 1529;
(c) Q. Hu, A.S. Hinman, Anal. Chem. 72 (2000) 3233;
(d) G. Niaura, A.K. Gaigalas, V.L. Vilker, J. Raman Spectrosc. 28 (1997) 1009.
[52] C. Turro, C.Y. Chung, N. Leventis, M.E. Kuchenmeister, P.J. Wagner, G.E. Leroi, Inorg. Chem. 35 (1996) 5104.
[53] J.R. Schoonover, K.M. Omberg, J.A. Moss, S. Bernhard, V.J. Malueg, W.H. Woodruff, T.J. Meyer, Inorg. Chem. 37 (1998) 2585.
[54] C.-Y. Lin, T.G. Spiro, Inorg. Chem. 35 (1996) 5237.
[55] (a) J.T. Hupp, R.D. Williams, Acc. Chem. Res. 34 (2001) 808, and references therein;
(b) C.A. Bignozzi, R. Argazzi, G. Strouse, J.R. Schoonover, Inorg. Chim. Acta 275 (1998) 380;
(c) R.G.H. Clarke, J. Mol. Struct. 113 (1984) 117;
(d) R.C. Rocha, M.G. Brown, C.H. Londergan, J.C. Salsman, C.P. Kubiak, A.P. Shreve, J. Phys. Chem. A 109 (2005) 9006.
[56] (a) M.B. Robin, P. Day, Adv. Inorg. Chem. Radiochem. 10 (1967) 247;
(b) K.D. Demadis, C.M. Hartshorn, T.J. Meyer, Chem. Rev. 101 (2001) 2655;
(c) N.S. Hush, Prog. Inorg. Chem. 8 (1967) 391;
(d) N.S. Hush, Electrochim. Acta 13 (1968) 1005.
[57] S. Bykov, I. Lednev, A. Ianoul, A. Mikhonin, C. Munro, S.A. Asher, Appl. Spectrosc. 59 (2005) 1541.
[58] A. Sato, Y. Mizutani, Biochemistry 44 (2005) 14709.
[59] (a) J. Terner, M.A. El-Sayed, Acc. Chem. Res. 18 (1985) 331;
(b) J.J. Turner, M.W. George, F.P.A. Johnson, J.R. Westwell, Coord. Chem. Rev. 125 (1993) 101;
(c) P. Glyn, M.W. George, P.M. Hodges, J.J. Turner, J. Chem. Soc. Chem. Commun. (1989) 1655;
(d) J.R. Schoonover, G.E. Strouse, Chem. Rev. 98 (1998) 1335.
[60] (a) C. Hicks, G.Z. Ye, C. Levi, M. Gonzales, I. Rutenburg, J.W. Fan, R. Helmy, A. Kassis, H.D. Gafney, Coord. Chem. Rev. 211 (2001) 207;
(b) T.J. Meyer, Pure Appl. Chem. 58 (1986) 1193;
(c) B.Z. Shan, Q. Zhao, N. Goswami, D.M. Eichhorn, D.P. Rillema, Coord. Chem. Rev. 211 (2001) 117;
(d) V. Balzani, A. Juris, Coord. Chem. Rev. 211 (2001) 97.
[61] (a) R.F. Dallinger, W.H. Woodruff, J. Am. Chem. Soc. 101 (1979) 4391;
(b) P.G. Bradley, N. Kress, B.A. Hornberger, R.F. Dallinger, W.H. Woodruff, J. Am. Chem. Soc. 103 (1981) 7441.
[62] D.S. Caswell, T.G. Spiro, Inorg. Chem. 26 (1987) 18.
[63] C. Creutz, M. Chou, T.L. Netzel, M. Okumura, N. Sutin, J. Am. Chem. Soc. 102 (1980) 1309.
[64] W.R. Browne, N.M. O'Boyle, J.J. McGarvey, J.G. Vos, Chem. Soc. Rev. (2005) 641.
[65] W.R. Browne, N.M. O'Boyle, W. Henry, A.L. Guckian, S. Horn, T. Fett, C.M. O'Connor, M. Duati, L. De Cola, C.G. Coates, K.L. Ronayne, J.J. McGarvey, J.G. Vos, J. Am. Chem. Soc. 127 (2005) 1229.
[66] R.M. Stratt, M. Marioncelli, J. Phys. Chem. 100 (1996) 12981.
[67] C. Okabe, T. Nakabayashi, N. Nishi, T. Fukaminato, T. Kawai, M. Irie, H. Sekiya, J. Phys. Chem. A 107 (2003) 5384.
[68] H. Miyasaka, T. Nobuto, A. Itaya, N. Tamai, M. Irie, Chem. Phys. Lett. 269 (1997) 281.

[69] C. Brady, P.L. Callaghan, Z. Ciunik, C.G. Coates, A. Dossing, A. Hazell, J.J. McGarvey, S. Schenker, H. Toftlund, A.X. Trautwein, H. Winkler, J.A. Wolny, Inorg. Chem. 43 (2004) 4289.
[70] S. Schenker, P.C. Stein, A.J. Wolny, C. Brady, J.J. McGarvey, H. Toftlund, A. Hauser, Inorg. Chem. 40 (2001) 134.
[71] (a) H. Hamaguchi, T.L. Gustafson, Annu. Rev. Phys. Chem. 45 (1994) 593; (b) K. Iwata, S. Yamaguchi, H. Hamaguchi, Rev. Sci. Instrum. 64 (1993) 2140.
[72] D.W. McCamont, P. Kukura, R.A. Mathies, J. Phys. Chem. A 107 (2003) 8208.
[73] M. Yoshizawa, M. Kurosawa, Phys. Rev. A 61 (1999) 013808.
[74] M. Yoshizawa, H. Aoki, H. Hashimoto, Phys. Rev. B 63 (2001) 180301.
[75] F.S. Rondonuwu, Y. Watanabe, J.-P. Zhang, K. Furuichi, Y. Koyama, Chem. Phys. Lett. 357 (2002) 376.
[76] F. Rosca, A.T.N. Kumar, X. Ye, T. Sjodin, A.A. Demidov, P.M. Champion, J. Phys. Chem. 104 (2000) 4280.
[77] F. Rosca, A.T.N. Kumar, D. Ionascu, X. Ye, A.A. Demidov, T. Sjodin, D. Wharton, D. Barrick, S.G. Sligar, T. Yonetani, P.M. Champion, J. Phys. Chem. 106 (2002) 3540.
[78] J.C. Polanyi, A.H. Zewail, Acc. Chem. Res. 28 (1995) 119.
[79] J.L. McHale, Acc. Chem. Res. 34 (2001) 265.
[80] (a) G.H. Czerlinski, M. Eigen, Z. Elektrochem. Angew. Phys. Chem. 63 (1959) 652;
(b) M. Eigen, Pure Appl. Chem. 6 (1963) 97.
[81] W. Wang, A. Demidov, X. Ye, J.F. Christian, T. Sjodin, P.M. Champion, J. Raman Spectrosc. 31 (2000) 99.
[82] L. Dhar, J.A. Rogers, K.A. Nelson, Chem. Rev. 94 (1994) 157.
[83] P.M. Champion, F. Rosca, D. Ionascu, W.X. Cao, X. Te, Faraday Discuss. 127 (2004) 123.
[84] D.W. McCamant, P. Kukura, R.A. Mathies, Appl. Spectrosc. 57 (2003) 1317.
[85] P. Kukura, D.W. McCamant, S. Yoon, D.B. Wandschneider, R.A. Mathies, Science 310 (2005) 1006.
[86] P.M. Champion, Science 310 (2005) 980.
[87] G.R. Fleming, Chemical Applications of Ultrafast Spectroscopy, Clarendon Press, Oxford, 1986, p. 147.
[88] K. Ishii, H. Hamaguchi, Chem. Phys. Lett. 367 (2003) 672.
[89] J.K. McCusker, Acc. Chem. Res. 36 (2003) 876.